Sequential poly-ubiquitylation by specialized conjugating enzymes expands the versatility of a quality control ubiquitin ligase

Weber, A. and Cohen, I. and Popp, O. and Dittmar, G. and Reiss, Y. and Sommer, T. and Ravid, T. and Jarosch, E.

Molecular Cell
2016 SEP 01 ; 63(5): 827-839
2016 AUG 25 (first published online)
doi: 10.1016/j.molcel.2016.07.020

Publisher: Cell Press / Elsevier

Sequential poly-ubiquitylation by specialized conjugating enzymes expands the versatility of a quality control ubiquitin ligase

Annika Weber[1,5], Itamar Cohen[2,5], Oliver Popp[3], Gunnar Dittmar[3], Yuval Reiss[2], Thomas Sommer[1,4], Tommer Ravid[2] and Ernst Jarosch[1]

[1] Intracellular Proteolysis, Max-Delbrueck-Center for Molecular Medicine, 13125 Berlin, Germany

[2] Department of Biological Chemistry, The Hebrew University of Jerusalem, 91904 Jerusalem, Israel

[3] Mass Spectrometric Core Facility, Max-Delbrueck-Center for Molecular Medicine, 13125 Berlin, Germany

[4] Institute of Biology, Humboldt University Berlin, 10099 Berlin, Germany

[5] These authors contributed equally

Correspondence should be addressed to TS, TR or EJ (tsommer@mdc-berlin.de, tommer.ravid@mail.huji.ac.il or ejarosch@mdc-berlin.de)

Summary

The Doa10 quality control ubiquitin (Ub) ligase labels proteins with uniform lysine 48-linked poly-Ub (K48-pUB) chains for proteasomal degradation. Processing of Doa10 substrates requires the activity of two Ub conjugating enzymes. Here we show that the non-canonical conjugating enzyme Ubc6 attaches single Ub molecules not only to lysines but also to hydroxylated amino acids. These Ub moieties serve as primers for subsequent poly-ubiquitylation by Ubc7. We propose that the evolutionary conserved propensity of Ubc6 to mount Ub on diverse amino acids augments the ubiquitylation sites within a substrate and thereby increases the target range of Doa10. Our work provides new insights on how the consecutive activity of two specialized conjugating enzymes facilitates the attachment of poly-Ub to very heterogeneous client molecules. Such stepwise ubiquitylation reactions most likely represent a more general cellular phenomenon that extends the versatility, yet sustains the specificity of the Ub conjugation system.

Introduction

An enzymatic cascade involving three types of enzymes promotes the conjugation of ubiquitin (Ub) to proteins: Initially, Ub activating enzyme (E1) forms a labile thio-ester bond with the carboxy-terminus of Ub, which is then transferred to a thiol group at the active site of an Ub conjugating enzyme (E2). Finally, Ub ligases (E3 enzymes) recruit client proteins to the vicinity of the E2 and facilitate the conjugation of Ub via its carboxy-terminal glycine to acceptor site(s) within the substrate (Hershko and Ciechanover, 1998; Metzger et al., 2014; Ye and Rape, 2009). In most cases, Ub is ligated to ε-amino groups of lysine side chains in the target protein. However, non-

canonical Ub conjugation at the amino-terminus (α-amino groups), thiol groups of cysteines and hydroxyl groups of serine and threonine residues have also been reported (McDowell and Philpott, 2016). Regardless of the initial Ub conjugation site, additional Ub moieties are then consecutively added through one of seven internal lysine residues or through the amino-terminus of Ub to form Ub polymers. The type of Ub-Ub linkage within a poly-Ub chain determines the cellular fate of the Ub-conjugated protein (Komander and Rape, 2012). For example, lysine 48-linked poly-Ub (K48-pUb) chains mediate recognition by the 26S proteasome, thereby targeting client proteins for degradation. In most cases, the type of Ub-Ub linkage is determined by the activity of the E2 enzyme (Ye and Rape, 2009). Yeast express 11 Ub conjugating enzymes with highly conserved catalytic domain, which is variable in size and enzymatic properties. The number of mammalian E2s in is considerably larger.

Mechanistically, the poly-ubiquitylation reaction can be divided into two distinct steps: The initial attachment of primary Ub to an acceptor site within the E3-bound substrate (priming), followed by consecutive additions of Ub molecules to primary Ub moieties (elongation). Since the mounting of the initial Ub is a pre-requisite for subsequent chain elongation, the availability of primary Ub conjugation sites is a critical determinant for poly-ubiquitylation. Given the large diversity of potential substrates, the requirements for an E2 that primes a target protein for ubiquitylation are most likely different from those of an E2 that catalyzes repeated cycles of a specific type of Ub-Ub linkage during chain elongation. Consequently, conjugating enzymes of the priming type must be able to identify promiscuous Ub ligation sites in large set of heterogeneous peptide environments, whereas the elongating enzymes should merely synthesize homogenous poly-Ub chains on a primary Ub. Indeed, several *in*

vitro studies suggest that individual Ub conjugating enzymes of the same E3 ligase complex assume distinct functions in the course of poly-Ub chain formation (Fletcher et al., 2015; Rodrigo-Brenni and Morgan, 2007; Wu et al., 2010).

Yeast Doa10 is a protein quality control (PQC) RING-finger-type Ub ligase that resides in the endoplasmic reticulum and the nuclear membrane (Deng and Hochstrasser, 2006; Swanson et al., 2001). Client proteins of Doa10 are decorated with K48-pUb chains and delivered to the 26S proteasome for degradation. Genetic data imply that Doa10 requires two distinct E2 enzymes, termed Ubc6 and Ubc7, for efficient substrate processing (Chen et al., 1993). *In vitro*, Ubc7 rapidly catalyzes K48-pUb, whereas the catalytic properties of Ubc6 remain mostly obscure (Bagola et al., 2013; Xu et al., 2009). Overexpression of Ubc6 in yeast impairs the degradation of a target protein to an extent similar to that observed in *UBC6*-deleted cells (Lenk et al., 2002; Sommer and Jentsch, 1993), suggesting that a balanced activity of these E2s is required for efficient substrate processing.

In light of the apparent dual E2 requirement for Doa10-mediated degradation, we set out to investigate the individual roles of Ubc6 and Ubc7. Here we show that Ubc6 and Ubc7 operate in tandem in the ubiquitylation of Doa10 substrates: Initially, Ubc6 attaches low molecular weight Ub moieties to proteins that are then elongated by Ubc7 to form K48-pUb chains. Notably, Ubc6, like its human orthologue UBE2J2 (Wang et al., 2009), not only mounts Ub via an isopeptide bond on lysine side chains but also ligates Ub to serine and possibly threonine residues via an oxy-ester bond. We propose that these properties of Ubc6 increase the availability of poly-ubiquitylation sites in target proteins and consequently ensure productive poly-Ub conjugation of Doa10 substrates. Tandem E2 activities, operating with a single E3 Ub ligase, probably contribute to efficient substrates ubiquitylation in other cellular

processes, and hence represent a common functional adaptation of the Ub conjugation system to target highly diverse protein populations (Fletcher et al., 2015; Rodrigo-Brenni and Morgan, 2007; Wu et al., 2010).

Results

Distinct roles for Ubc6 and Ubc7 in the *in vivo* ubiquitylation of a Doa10 substrate

Degradation of Doa10 substrates, such as Vma12-*DegAB* (Alfassy et al., 2013), is impaired to a similar extent in yeast cells devoid of the Ub conjugating enzymes Ubc6 or Ubc7 or the Ub ligase Doa10 (**Figure 1A**). Evidently, each of the E2 enzymes is absolutely required for this process, suggesting a cooperative mode of action. To assess the distinct functions of Ubc6 and Ubc7 in substrate ubiquitylation, we isolated Vma12-*DegAB* from cells and determined its ubiquitylation pattern. We find that in *wild type* yeast cells Vma12-*DegAB* is profoundly poly-ubiquitylated, whereas in strains deleted for *UBC6* (*ubc6Δ*) or *DOA10* (*doa10Δ*) Vma12-*DegAB* ubiquitylation is barely detectable (**Figure 1B**). The protein is still ubiquitylated in cells lacking Ubc7, (*ubc7Δ*), albeit to a substantially lower extent. Apparently, Ubc6 is capable of attaching Ub even in the absence of Ubc7 but it is insufficient to initiate degradation. Consistently, a ubiquitylated species that migrates on gels at a position corresponding to mono-ubiquitylated Vma12-*DegAB* also accumulates in *ubc7Δ* cells (**Figure 1B**; arrowheads). We next monitored the ubiquitylation pattern of Vma12-$DegAB_{DD}$, a variant where two adjacent leucine residues at the carboxy-terminus are replaced with aspartic acid residues. The resulting protein is conjugated to Ub but is not subjected to proteasomal degradation (Furth et al., 2011) resulting in an elevated steady state level of the poly-ubiquitylated mutant protein (Alfassy et al., 2013).

Hence, monitoring Vma12-*DegAB*$_{DD}$ poly-ubiquitylation enables comparative exploration of Ub conjugation by the Doa10 pathway, which is uncoupled from subsequent proteasomal degradation. Consequently, we find mono-ubiquitylated Vma12-*DegAB*$_{DD}$ in *ubc7*Δ cells and to a lesser extent, in *wild type* cells (**Figure 1C**). The overexpression of Ub lacking lysine 48 (Ub$_{R48}$) substantially diminishes the amount of poly-ubiquitylated Vma12-*DegAB*$_{DD}$ and increases low molecular weight ubiquitylated species, including mono-ubiquitylated Vma12-*DegAB*$_{DD}$. Similar expression of Ub lacking lysine 11 (Ub$_{R11}$) only marginally affects ubiquitylation (**Figure 1D**). To figure if K48-linked Ub also contributes to the buildup of poly-Ub in *ubc7*Δ cells, we tested Vma12-*DegAB* ubiquitylation profile in *ubc7Δ* cells overexpressing either *wild type* Ub or Ub$_{R48}$. The *ubc7Δ* cells also expressed defective Rpt4 and thus were also inhibited for proteasomal degradation (Meusser and Sommer, 2004). As shown in **Figure S1A**, Vma12-*DegAB* ubiquitylation is markedly inhibited in *ubc7Δ* cells or in *wild type* cells overexpressing Ub$_{R48}$ while the expression of Ub$_{R48}$ in *ubc7*Δ cells does not cause a further significant reduction. In agreement with these findings, mass spectrometric analysis of Vma12-*DegAB* isolated from *wild type* yeast cells detected lysine 48-linked Ub but no lysine 63- or lysine 11-linked forms (**Figure S1B**). Furthermore, Vma12-*DegAB* purified from *UBC6*- or *UBC7*-deleted strains contains substantially less K48-pUb (**Figure S1B**). Together, these findings indicate that Ubc6-mediated ubiquitylation alone cannot induce significant proteasomal degradation and that Ubc7-mediated K48-pUb chain formation on substrates strongly depends on Ubc6.

Distinct *in vitro* activities of Ubc6 and Ubc7

The mutual requirement for Ubc6 and Ubc7 during K48-pUb chain formation on Vma12-*DegAB* implies that they fulfill distinct functions. Based on our preliminary ubiquitylation assays, we speculated that Ubc6-conjugated Ub moieties are necessary to target subsequent poly-ubiquitylation by Ubc7. To test this hypothesis, we employed an *in vitro* ubiquitylation assay that measures the activity of the E2 enzymes. The assay contained various compositions of the following components: The catalytically important RING-finger domain of Doa10 (Doa10R) (Cohen et al., 2015), Ubc7, the cytosolic domain of the Ubc7 activator Cue1 (Cue1ΔTM) (Bazirgan and Hampton, 2008), the cytosolic part of Ubc6 (Ubc6ΔTM) and Ub (**Figure S2A**). The ubiquitylation reaction was initiated by the addition of an Ub activating enzyme (E1) and ATP. The *in vitro* assay results show that in the presence of Cue1ΔTM, Ubc7 readily assembles unanchored Ub chains in a time dependent manner (**Figure 2A** (Bagola et al., 2013)) but does not mount Ub on Doa10R. In contrast, Ubc6ΔTM promotes the attachment of single Ub moieties to itself and to Doa10R, but barely to free Ub (**Figure 2B**). Most importantly, Doa10R is poly-ubiquitylated only when both Ubc6ΔTM and Ubc7/Cue1ΔTM are present in the reaction (**Figure 2C and Figure S2B**).

Self-ubiquitylation is a common property of E3 RING finger domains, when incubated in *in vitro* ubiquitylation reactions with their cognate E2 enzymes (Lorick et al., 1999). Consequently, E3 self-ubiquitylation assays have served to characterize catalytic properties of E2 enzymes (Kim et al., 2007; Lorick et al., 1999). Consequently, we further employed the Doa10 RING domain to investigate the apparently distinct roles of Ubc6 and Ubc7 in the formation of poly-Ub chains. We find that Ubc6ΔTM promotes self- and Doa10R mono-ubiquitylation of *wild type* Ub as well as Ub_{R11},

Ub_{R48}, and Ub_{R63} (**Figure S2C**). In contrast, further Doa10R poly-ubiquitylation by Ubc7 is abrogated when *wild type* Ub is replaced by Ub_{R48} but not by Ub_{R11} or Ub_{R63}. These results confirm the absolute requirement for lysine 48 for Ub chain elongation (**Figure 2D**). The results are consistent with a tandem mode of action where initial mono-Ub conjugation by Ubc6ΔTM primes Doa10R for subsequent Ubc7 catalyzed K48-pUb chain formation

In vitro studies of Anaphase Promoting Complex (APC) mutants suggest that individual E2 enzymes that function in discrete steps of the poly-ubiquitylation reaction are differently activated by the APC11 RING subunit of this E3 ligase complex (Brown et al., 2014). Three of the amino acids in the APC11 RING domain that define one E2 interaction site are also conserved in the Doa10 RING-domain (**Figure 3A,** red circles). We therefore tested, if these amino acids affect functional interactions of Ubc6 and Ubc7 with the Doa10 RING domain. To this end, bacterially expressed Doa10 RING variants, harboring amino acid substitutions in the respective positions, were purified. We then tested Ubc6 and Ubc7-mediated ubiquitylation in the presence of the various Doa10 constructs (**Figures 3B and 3C**). The substitution of isoleucine 41 with alanine ($Doa10R_{A41}$) abolishes both the mono-ubiquitylation by Ubc6 and the formation of free poly-Ub chains by Ubc7, while the replacement of arginine 43 with alanine ($Doa10R_{A43}$) primarily affects the Ubc7 activity (**Figures 3B and 3C**). In contrast, alanine at position 73 ($Doa10R_{A73}$) selectively inhibits Ubc6 activity, while the synthesis of unanchored Ub chains by Ubc7 is barely affected (**Figures 3B and 3C**). Poly-ubiquitylation of the three Doa10R variants is substantially decreased in the presence of both E2 enzymes, most likely because each mutant limits at least one E2 (**Figure 3D**). Thus, in agreement with their distinct roles in the *in vitro* ubiquitylation reaction, both Ubc6 and Ubc7 functionally interact

through the same binding interface with Doa10R, albeit in a different fashion. Circular dichroism spectral analysis of the Doa10 mutants did not detect any structural perturbations (Figure S3) thus excluding the possibility that Doa10 structural perturbation, rather than disruption of specific amino acid interactions, affected E2 activities. Of note, *in vitro* auto-ubiquitylation of Ubc6 is does not require stimulation by Doa10R. Similar E3-independent ubiquitylation reactions were also reported for other E2 enzymes and thus appear to represent a common phenomenon (David et al., 2010).

Ubc7 forms K48-pUb chains on primary Ub moieties attached by Ubc6

To ascertain that initial attachment of Ub by Ubc6 triggers subsequent poly-ubiquitylation by Ubc7, we reconstituted the distinct E2 reactions in tandem. Accordingly, Doa10R was incubated with E1, ATP/Mg^{2+}, Ubc6ΔTM and either Ub_{R48} or $Ub_{R63,}$ after which Ubc6ΔTM was removed and Ubc7/Cue1ΔTM and excess of *wild type* Ub were added. As shown in **Figure 4A,** chain extension by Ubc7 occurs only on Doa10R that is initially conjugated to Ub_{R63} but to Ub_{R48}. Ubc7 by itself is capable of synthesizing unanchored Ub chains under all tested conditions, demonstrating that it is catalytically active in the assays (**Figure S4A**). Next, we wanted to confirm that Ubc7 directly synthesizes Ub chains on Ub moieties that are conjugated to a substrate. To this end, we purified Doa10R, which was mono-ubiquitylated *in vitro* by Ubc6 (Doa10R-Ub), and incubated it with Ubc7/Cue1ΔTM and Ub_{R48}. The employment of Ub_{R48}, allows only a single Ub to be ligated to Doa10R-Ub resulting in the formation of a Doa10R-di-Ub (Doa10R-Ub_2) product. Indeed, significant amounts of Doa10R-Ub are readily converted to a di-ubiquitylated form in an ATP-dependent manner, whereas prolonged incubation with Ubc6 does not increase the portion of

Doa10R-Ub_2 (**Figure 4B**). Mass spectrometry analysis of the Doa10R-Ub_2 adduct confirmed that the only Doa10R-Ub_2, generated by Ubc7/Cue1ΔTM, contains lysine 48-linked Ub, as previously reported (Bagola et al., 2013) (**Figures 4C and S4B**). Consistently, neither K63- nor K11- linked Ub-Ub adducts are detected in the MS-analyzed Doa10R-Ub_2 samples. Doa10R-Ub_2 in reactions without ATP or without Ubc7/Cue1ΔTM most likely represent double-mono-ubiquitylated Doa10R. Indeed, no Ub-Ub adducts were detected in these Doa10R-Ub_2 species. We thus confirm that Ubc7 extends the initial Ubc6-conjugated Ub by forming sequential Ub-K48 linkages. Notably, the cytoplasmic domain of UBE2J2, a human homologue of Ubc6, also promotes mono-ubiquitylation of Doa10, demonstrating that the catalytic properties of these enzymes are highly conserved in evolution (**Figure S5**).

Next, we sought to verify the tandem ubiquitylation mechanism by Ubc6 and Ubc7 in intact yeast cells. To this end, we adopted an approach previously employed to study the role of mono-Ub in vesicular trafficking (Haglund et al., 2003; Ramanathan et al., 2013). We reasoned that if mono-ubiquitylation by Ubc6 creates the poly-Ub site for Ubc7, then fusing Ub provides an intrinsic primary Ub site and thus facilitate substrate poly-ubiquitylation in the absence of Ubc6. Consequently, we expressed a chimeric protein between of Ub_{V76} and the amino-terminus of catalytically inactive $Ubc6_{S87}$ (Ub_{V76}-$Ubc6_{S87}$). The mutation in the carboxy-terminal di-glycine motif of Ub was designed to prevent internal cleavage of the fusion protein by Ub hydrolases (Butt et al., 1988; Johnson et al., 1992). Since the enzymatic activity of Ubc6 is required for Doa10-mediated ubiquitylation, the active site $Ubc6_{S87}$, is a stable protein (**Figure S4C** and (Swanson et al., 2001; Walter et al., 2001)). As anticipated, the Ub-E2 fusion protein, Ub_{V76}-$Ubc6_{S87}$, is rapidly degraded in *wild type* and in *ubc6*Δ cells but not in *Ubc7*Δ or *Doa10*Δ cells (**Figures 4D and S4D).** This confirms that Doa10-

mediated poly-ubiquitylation by Ubc7 merely requires a primary Ub acceptor that is inherently provided in Ub_{V76}-$Ubc6_{S87}$. The fact that a the hybrid protein $Ub_{R48,V76}$-$Ubc6_{S87}$ is not degraded, once again demonstrates the requirement for of lysine 48 of Ub as an internal acceptor site in Ub for Ubc7-mediated poly-ubiquitylation (**Figures 4E and S4E**). Altogether, these *in vivo* findings indicate that the attachment of Ub to an otherwise non-degradable Doa10 substrate is essential and sufficient for poly-ubiquitylation by Ubc7 and subsequent proteasomal degradation.

Ubc6 targets amino acids other than lysines as acceptor sites for Ub conjugation

Results from reconstitution experiments in cell lysates demonstrate that the human orthologue of Ubc6, UBE2J2, is capable of attaching Ub to the ε-amino groups of lysine residues via an isopeptide bond as well as to hydroxyl groups of serines and threonines via a pH-sensitive oxy-ester bond (Wang et al., 2009). To test whether Ubc6 similarly forms Ub-ester bonds, we examined the susceptibility of Ubc6 conjugates to high pH treatment. We observe a substantial reduction of mono-ubiquitylated Ubc6ΔTM, when NaOH is added after completion of the *in vitro* reactions (**Figure 5A**, compare lanes 5 and 6 and lanes 7 and 8). Analysis of the reaction products by mass spectrometry confirms the presence of a serine-Ub ester by a peptide species with a molecular mass corresponding to two penultimate di-glycine residues on serine 196 of Ubc6ΔTM (**Figures 5B and 5C**). Furthermore, substituting serine 196 with alanine substantially decreases the amount of auto-ubiquitylated Ubc6ΔTM, both *in vitro* (**Figure 5A**, compare lanes 3 and 4) and *in vivo* (**Figure 5D**). In agreement with our *in vitro* data (**Figures 3C and 5A**), the *in vivo* auto-ubiquitylation of Ubc6 is detectable in cells devoid of Doa10, indicating that the E3 enzyme is not obligatory for the stimulation of Ubc6 activity. Together, these

results demonstrate that Ubc6 can conjugate Ub to lysine as well as to serine and possibly threonine residues.

We further investigated, whether Ubc6 shows a bias towards lysine or serine/threonine ubiquitylation sites. To this end we conducted *in vitro* self-ubiquitylation assays where we measured the kinetics of pH-sensitive and pH-insensitive mono-Ub formation on Ubc6. The results presented in **Figure S6** confirm the accumulation of both NaOH-sensitive and -insensitive Ub-Ubc6 conjugates at short time points, indicating that Ubc6 does not display an apparent preference for the modification of lysines or serine/threonine acceptor sites. However, Ubc6 appears to be highly promiscuous in target site selection and therefore we observe differences in Ub conjugation kinetics at later time points. This indicates distinct accessibility of individual Ub acceptor sites or differences in the stability of the oxy-ester and isopeptide bonds in the assay (**Figure S6)**. Concordantly, the rate of degradation of $Ubc6_{A196}$ in yeast is similar to that of the *wild type* protein and its expression does not affect the degradation of other Doa10 substrates (**Figures S6B and S6C**). Apparently, serine 196 is not a crucial or a favorable poly- ubiquitylation site *in vivo*. Obviously, it is also not required for Ubc6 activity.

The tail-anchored protein Sbh2 (**Figures 6A)** becomes unstable in cells lacking its binding partner Ssh1 (Habeck et al., 2015). Turnover of Sbh2 under these conditions strongly depends on Doa10 and Ubc7 activities, whereas the disruption of *UBC6* only moderately affects proteolysis (**Figures 6B and S7A;** (Habeck et al., 2015)). This implies that a large proportion of Sbh2 is degraded independently of Ubc6. In contrast, the turnover of an Sbh2 variant, Sbh2Δ4K, that lacks four adjacent lysine residues in its cytosolic domain (**Figure 6A**, red dots**)**, strongly relies on Ubc6 function (**Figures 6C and S7A**). Intriguingly, a protein composed of un-cleavable Ub,

fused to the amino-terminus of Sbh2Δ4K (Ub_{V76}-Sbh2Δ4K), is degraded in *ubc6*Δ cells, indicating that the amino-terminal Ub bypasses the requirement for Ubc6 (**Figures 6D and S7B**). These findings further support a critical role of Ubc6-mediated priming for efficient ubiquitylation of Doa10 substrate proteins. We also find a good correlation between the turnover of FLAG-Sbh2 and FLAG-Sbh2Δ4K and their ubiquitylation levels (**Figures 6E and S7C**): FLAG-Sbh2 is ubiquitylated to a comparable extent in *wild type* and *ubc6*Δ cells, while FLAG-Sbh2Δ4K ubiquitylation is significantly reduced in *ubc6*Δ cells. Importantly, ubiquitylation of FLAG-Sbh2Δ4K is sensitive while that of FLAG-Sbh2 is resistant to high pH treatment (**Figure 6F**, compare lanes 2 and 3 with lanes 5 and 6, **Figure S7D**). These *in vivo* observations support our hypothesis that, when appropriate lysine residues are available, Ubc7 can directly poly-ubiquitylate selected substrates. On the other hand, Ubc6 is less stringent in selecting suitable Ub conjugation sites and readily attaches Ub to amino acids other than lysines. This unique property of Ubc6 turns critical for the poly-ubiquitylation and subsequent proteasomal degradation of proteins such as Sbh2Δ4K, where lysine side chains are not readily available.

Discussion

In this study we demonstrate that efficient ubiquitylation and subsequent proteasomal degradation of Doa10 client proteins requires the successive activity of two highly specialized Ub conjugating enzymes (**Figure 7**). In the priming step, Ubc6 conjugates low molecular weight Ub moieties to Doa10 substrates, after which Ubc7 elongates the Ub-primer to form K48-pUb chains. These conclusions are based on the following observations: (a) In yeast cells, Doa10 substrates require both Ubc6 and Ubc7 for efficient poly-ubiquitylation and degradation (**Figure 1**). (b) Both *in vivo*

and *in vitro* protein ubiquitylation assays indicate that high molecular weight poly-Ub-substrate conjugates only form in the presence of both E2s. Ubc6 alone forms low molecular weight Ub-protein conjugates whereas in the absence of Ubc6, Ubc7 rarely assembles Ub conjugates on Doa10 substrates (**Figures 1 and 2**). (c) The reconstitution of partial Ubc6 and Ubc7 ubiquitylation reactions in tandem and the use of Ub-lysine mutants, both *in vivo* and *in vitro*, indicate that Ubc7 extends the primary Ubc6-conjugated by forming lysine-48 linked poly-Ub chains (**Figure 1 and Figure 4**). (d) The tandem poly-ubiquitylation mechanism is confirmed *in vivo* by demonstrating that Ubc6 priming is not required for a hybrid Ub-Doa10 substrate that is efficiently poly-ubiquitylated by Ubc7 alone (**Figures 4 and 6**). We further show that for efficient poly-ubiquitylation, both E2 enzymes must functionally interact with the Doa10 RING domain (**Figure 3**). Poly-ubiquitylation processes involving the consecutive activity of distinct E2 enzymes were previously postulated from *in vitro* reconstitution studies on the APC and $SCF^{\beta TrCP2}$ UB ligase complexes, on the auto-ubiquitylation of the RING-finger ligase BRCA1, as well as on the function of TRIM21 at the immune system (Christensen et al., 2007; Fletcher et al., 2015; Rodrigo-Brenni and Morgan, 2007; Wu et al., 2010). Still, to our knowledge this study is the first to show the biological relevance of such tandem ubiquitylation by demonstrating its requirement for the sequential activity of Ubc6 and Ubc7 during processing of Doa10 PQC client proteins in yeast cells.

In contrast to substrates of regulated protein turnover, polypeptides subjected to PQC exhibit a large variety in sequence composition and structural properties (Ravid and Hochstrasser, 2008). Accordingly, tandem ubiquitylation mechanisms may have evolved to facilitate Ub conjugation in highly diverse protein landscapes (Mattiroli and Sixma, 2014). For example, yeast Ubc6 is required for efficient degradation of Doa10

substrates (Chen et al., 1993). However, this enzyme, by itself, is unable to generate poly-Ub chains for the recognition by 26S proteasomes (Xu et al., 2009). Consequently, its detailed role in proteasomal degradation remained enigmatic. We now find that Ubc6 conjugates single Ub moieties to client proteins that then serve to initiate poly-ubiquitylation by Ubc7. The formation of non-canonical Ub conjugates by Ubc6 facilitates the establishment of multiple mono-Ub sites, which in turn increases the likelihood of productive poly-ubiquitylation. This becomes evident by the large proportion of Ubc6-generated primary Ub conjugates that are sensitive to high pH and thus represent ester bonds with hydroxyl group-containing amino acid side chains (**Figure 5**). Indeed, we detect serine-Ub conjugated species in mass spectrometric analysis. This unique ability of Ubc6 to target non-canonical Ub acceptor sites prompts the degradation of a substrate that does not harbor accessible lysine residues (Sbh2Δ4K; **Figure 6**). The mammalian Ubc6 orthologue UBE2J2 can also prime proteins for Ubc7-mediated poly-ubiquitylation (**Figure S5**) and was shown in a reconstituted system to attach Ub to amino acids other than lysines (Wang et al., 2009). Intriguingly, ubiquitylation of the non-secreted immunoglobulin light chain NS-1, a natural ERAD substrate of the Hrd1 ligase in mammals, occurs on lysine as well as serine and threonine residues, although the E2(s) involved in this process are not known (Shimizu et al., 2010). Moreover, degradation of MHC class I molecules via Hrd1 and UBE2J1, an additional mammalian Ubc6 homologue, and turnover of T-cell Antigen Receptor α-Chain involves the ubiquitylation of non-lysine residues within the substrate (Burr et al., 2013; Yu and Kopito, 1999). Finally, recent studies of the degradation of the yeast E3 ligase Asi2 by the Doa10 pathway revealed NaOH-sensitive ubiquitylation of a lysine-less version of the protein (Boban et al., 2015). These findings support the notion that

the modification of hydroxylated amino acids with Ub is a common event during ERAD and possibly also other degradative processes.

Both, the flexibility in Ub conjugation sites selection and the inability to form Ub chains, may be attributed to the unique properties of the active site domains of Ubc6 and its mammalian orthologues (Lester et al., 2000). The evolutionary conserved features of these proteins most likely reflects an important function in PQC systems that has possibly evolved to salvage degradation of polypeptides containing few or no accessible lysine residues and that therefore cannot be efficiently processed by canonical E2 enzymes.

In contrast to Ubc6, Ubc7 is extremely proficient in forming lysine 48-linked Ub chains (Bagola et al., 2013) but is less capable to attach Ub to other proteins. The activity of Ubc7 is largely governed by binding to its partner protein Cue1, probably to prevent uncontrolled ubiquitylation and substrate degradation (Bagola et al., 2013; Bazirgan and Hampton, 2008; Biederer et al., 1997; Kostova et al., 2009; Metzger et al., 2013; Ravid and Hochstrasser, 2007). Both the requirement for preceding Ubc6-mediated priming in the Doa10 ligase pathway and the unique E2 binding sites on the E3 RING finger domain constitute additional regulatory elements for the activity of Ubc7. This elaborate mechanism may prevent erroneous poly-ubiquitylation reactions by other E2 enzymes such as Mms2/Ubc13 that mounts Ub-chains linked through lysines other than K48 on mono-ubiquitylated proteins (Hoege et al., 2002). Remarkably, Ubc7 is capable of directly poly-ubiquitylating client proteins of the yeast Hrd1 Ub ligase (Bays et al., 2001; Hirsch et al., 2009). In this case, access of Ubc7 to appropriate conjugation sites may be facilitated by the partial unfolding of Hrd1 substrates prior to their extraction from the endoplasmic reticulum. Furthermore, Ubc7 is activated differently by the RING domains of Hrd1 and Doa10 suggesting a

particular alignment of Ubc7 towards the Hrd1 ligase, which in turn may promote direct transfer of Ub to acceptor sites within the substrate (Cohen et al., 2015).

Recent studies indicate that the functional engagement of multiple E2 enzymes with a single E3 ligase is not restricted to protein quality control (Christensen et al., 2007; Fletcher et al., 2015; Rodrigo-Brenni and Morgan, 2007; Wu et al., 2010). Obviously, all Ub conjugating enzymes display unique properties regarding their preferences to interact with individual Ub ligases and their capability to catalyze substrate-Ub or certain types of Ub-Ub linkages. In addition, some E2s are exclusively found at destined cellular locations. Our study now suggests that the subsequent activity of specialized conjugating enzymes in certain poly-ubiquitylation reactions most likely represents a functional adaptation to ensure the availability of poly-Ub sites and thereby contributes to the flexibility of the Ub system.

Experimental Procedures

Antibodies.

Monoclonal antibodies against Ub (P4D1, sc-8017 Santa Cruz Biotechnology, dilution 1: 1,000), FLAG (F3169 Sigma, dilution 1: 1,000) and HA (H9658, Sigma-Aldrich, dilution 1: 5,000) were commercially available. Polyclonal antibodies against Doa10 (1:30,000), Ubc6 (*in vitro*: 1:10;000; *in vivo*: 1: 2,000), Sec61 (1: 5,000), Ubc7 (1: 10,000) and Sbh2 (1: 1,000) were described (Bagola et al., 2013; Finke et al., 1996; Gauss et al., 2006; Neuber et al., 2005; Walter et al., 2001). A poly-clonal rabbit anti-Myc antibody was purchased from Cell Signaling Technology (71D10). Horseradish peroxidase-coupled secondary antibodies were diluted 1:10,000 (Sigma-Aldrich, A9044 (anti-mouse), A0545 (anti-rabbit), P8651 (Protein A-Peroxidase)) and

used for enhanced chemiluminescence detection with a LI-COR Odyssey system. Fluorescently labeled secondary antibodies (IRDye®800CW anti-rabbit, LI-COR) were diluted 1: 20,000 and visualized with a LI-COR Odyssey system.

Yeast strains and plasmids.

All yeast strains were haploid decedents of DF5 (genotype: *MATa/alpha trp1-1(am)/trp1-1(am) his3-Δ200/his3-Δ200 ura3-52/ura3-52 lys2-801/lys2-801 leu2-3,-112/ leu2-3,-112*) that were generated following standard protocols for transformation or crossing. They are listed in **Table S1**. Plasmids listed in **Table S2** were generated by amplifying fragments of yeast genomic DNA by polymerase chain reaction (PCR) using PfuUltra (Stratagene) or Expand (Sigma-Aldrich) polymerase with appropriate oligonucleotides and transferring them into the given vectors by cloning via restriction sites or by the use of the Transfer PCR technique (Erijman et al., 2014). Constructs containing point mutations were generated using the QuikChange site directed mutagenesis kit (Aligent Technologies) following the manufacturer's instructions. The identity of all plasmids was verified by sequencing.

Preparation of recombinant proteins.

GST fusion proteins were expressed and purified following a recently published protocol (Bagola et al., 2013). Doa10R variants were further purified on a Superdex 75 size exclusion column (GE Healthcare) in a 20 mM HEPES buffer (pH 7.5). Human Uba1 (Ub activating enzyme; E1) and FLAG-Ub were obtained as described elsewhere (Berndsen et al., 2013; Berndsen and Wolberger, 2011). For purification of His-tagged proteins *E.coli* M15 cells were transformed with the appropriate plasmids and cultivated in LB-media at 37 °C to an optical density of 0.8. Protein expression was induced by addition of 0.5 mM IPTG for 4 hours. Cells were pelleted and lyzed in

a French Press system (AVESTIN) in buffer containing 50 mM $NaHPO_4$ (pH 7.5), 300 mM NaCl, 15 mM imidazole and protease inhibitor (cOmplete™, EDTA-free, Roche). TALON® Resin (Clontech) was added and the samples were incubated at 4 °C for 2.5 hours to isolate His-tagged proteins. For the elution of the proteins imidazole was added to a concentration of 300 mM. Proteins were concentrated and stored at -80 °C.

In vitro ubiquitylation assay.

A Coomassie-stained gel showing the purified proteins for the *in vitro* ubiquitylation assay is given in Supplementary Figure S1A. Equal amounts (3.5 µM) of Ubc6ΔTM variants, Ubc7/Cue1ΔTM, Doa10R variants were incubated with 7.5 µM Ub and 150 nM Uba1 (E1) in a buffer containing 50 mM HEPES (pH 7.5), 2.5 mM Magnesium acetate and 0.5 mM Dithiothreitol (DTT). The reaction was started by the addition of ATP to a concentration of 4 mM and incubated for 20 min at 30 °C. Reactions were stopped by adding sample buffer containing DTT and analyzed by SDS-PAGE and immunoblotting. Aliquots representing time point 0 were removed before the addition of ATP. Ub_{R11}, Ub_{R48} and Ub_{R63} were purchased from Boston Biochem. Ub_{C20} was labeled with Alexa488 as described recently (Bagola et al., 2013).

Immunoprecipitation of Doa10R.

Doa10R was isolated from *in vitro* ubiquitylation reactions by adding 15 volumes IP buffer (50 mM Tris (pH 7.5), 150 mM NaCl, 5 mM EDTA, 1 % Triton, 0.1 % SDS) and a mixture of anti-Doa10 antibody and protein A Sepharose (GE Healthcare). After incubation at 4 °C overnight the resin was washed, proteins were eluted with DTT containing sample buffer and analyzed by SDS-PAGE and immunoblotting.

Purification of mono-ubiquitylated Doa10R.

200 µM Doa10R was incubated with 200 µM Ubc6ΔTM-His_6, 600 µM Ub, 0.5 µM E1 and 10 mM ATP in a final volume of 2.5 mL reaction buffer (50 mM HEPES (pH 7.5), 6.5 mM Magnesium acetate and 0.5 mM DTT) for 16 h at 30 °C. The reaction was diluted to 10 ml with buffer containing 50 mM $NaHPO_4$ (pH 7.5), 300 mM NaCl, 15 mM imidazole and incubated with 500 µL TALON® Resin (Clontech) for 1 h at room temperature to remove Ubc6ΔTM-His_6. Doa10R-Ub was then purified from the supernatant by size exclusion chromatography on a Superdex 75 column (GE Healthcare). Of note, this Doa10R-Ub preparation still contained minor amounts of Ubc6ΔTM-His_6 and Doa10R. Residual Ubc6ΔTM-His_6 in the sample was inactivated by the addition of 20 mM N-ethylmaleimide (NEM) and incubation for 1 h at room temperature. NEM was then removed by dialysis against 20 mM HEPES buffer. *In vitro* ubiquitylation experiments with Doa10R-Ub were performed as described above.

Sample preparation for mass spectrometry

Proteins separated by SDS-PAGE were processed for mass spectrometric analysis as described (Shevchenko et al., 2006). Briefly, gel pieces were washed with 50 % ethanol in 50 mM ammonium bicarbonate (ABC) and 50 mM ABC in an alternating fashion. Disulfide bonds were reduced by the addition of 2.5 pmol Tris-(2-carboxyethyl) phosphine (TCEP) and alkylated by adding 12.5 pmol chloroacetamide both for 30 min at room temperature followed by a 10 h digest with 5 µg sequencing grade Trypsin (Promega). Peptides were extracted with extraction buffer (80 % acetonitrile, 20 mM acetic acid) and subsequently dried in a Speed-Vac (Savant). Purification on C18 stage-tips (Rappsilber et al., 2007) was done in 20 mM acetic

acid to preserve Ub-ester bonds. The eluted peptides were dried in a Speed-Vac and dissolved in 3 % acetonitrile, 20 mM acetic acid.

Liquid chromatography tandem mass spectroscopy (LC-MS/MS)

Samples were measured with an LTQ orbitrap VELOS mass spectrometer (Thermo) connected to a Proxeon nano-LC system (Thermo). 5 µl of the sample were loaded on a nano-LC column (0.074 mm x 250 mm, 3 µm Reprosil C18, Dr Maisch GmbH) and separated by a 155 min gradient (4 to 76 % acetonitrile) a flow rate of 0.25 µl/min, ionized on a proxeon ion source and sprayed directly into the mass spectrometer. MS acquisition was done at a resolution of 60'000 with a scan range from 200 to 1700 m/z in FTMS mode selecting the top 20 peaks for CID fragmentation. MS/MS scans were measured in IT mode with an isolation width of 2 m/z and a normalized collision energy of 40 eV. Dynamic exclusion was set to 60 s. For data analysis the MaxQuant software package version 1.5.2.8 (Cox and Mann, 2008) was used with Carbamidomethylation set as a fixed and oxidized methionine and acetylated amino-termini as variable modifications. A monoisotopic mass-shift of 114.042927 Da corresponding to the addition of a double-glycine (tryptic carboxy-terminal fragment of Ub) was set as a variable modification on lysine, serine, threonine and cysteine residues. An FDR of 0.01 was applied for peptides and proteins and the search was performed using the *S. cerevisiae (S288c)* Uniprot database (August 2014).

Ubiquitin chain quantification

The proteins were isolated from gels and digested into peptides as described above. Purified material was supplemented with a mixture of heavy-labeled reference peptides (500 fmol each; **Table S3**) for the quantification of the different Ub linkage

types. The samples were loaded onto a 15 cm reverse phase column (3 µm Reprosil C18-beads, Dr. Maisch GmbH, packed in house) and eluted with a 1 h 4% to 76% Acetonitrile gradient. The separated peptides were ionized and directly infused into a Q-TRAP 5500 (ABSciex) mass-spectrometer and the linkage specific peptides were monitored as described elsewhere (Mirzaei et al., 2010). Peak areas were integrated using the MultiQuant 2.0 software package (ABSciex). For further analysis and statistical tests the R-Software package (www.r-project.org) was used.

Cycloheximide decay assay.

Yeast cells in log-phase were re-suspended in SD-media and cycloheximide (Sigma; final concentration 100 µg ml^{-1}) was added. Aliquots were removed at indicated time points and NaN_3 was added to a concentration of 10 mM. Total cell lysates were prepared from the samples and analyzed by SDS-PAGE and immunoblotting. For quantification of protein turnover, immunoblots were incubated with fluorescently labeled secondary antibodies and analyzed on a LI-COR Odyssey system.

In vivo ubiquitylation of Vma12-DegAB and FLAG-Sbh2.

Ubiquitylation of Vma12-*DegAB* in cells was determined as previously described (Furth et al., 2011). FLAG-Sbh2 variants were isolated from yeast cells overexpressing Myc-tagged Ub. Cells in exponential growth phase were harvested and lysed with glass beads in buffer containing 6 M urea, 50 mM Tris pH 7.5, 150 mM NaCl, 1 % SDS, 1 mM PMSF and 20 mM NEM. The lysate was diluted with 9 volumes of IP dilution buffer (55 mM Tris pH 7.5, 165 mM NaCl, 5.5 mM EDTA, 1.1 % Triton, 1 mM PMSF and 20 mM NEM) and cleared from cell debris by centrifugation (20,000 x g, 10 min, 4 °C). 50 µL ANTI-FLAG®M2 Affinity Gel (Sigma-Aldrich) was added and incubated overnight at 4 °C. After washing, the beads were

treated with SDS-PAGE sample buffer for 15 min at 42 °C. The supernatant was collected and 100 mM DTT and, where indicated, NaOH (final concentration 150 mM) or water were added and heated for another 15 min at 65 °C. Samples were separated on SDS-PAGE and analyzed by immunoblotting.

Author Contributions

AW, IC, OP, YR and EJ performed experimental work. All authors designed experiments and discussed the results. AW, IC, TR and EJ wrote the manuscript.

Acknowledgements

The authors want to thank the members of the Dittmar, Ravid and Sommer groups and Jasmin Schlotthauer for support and fruitful discussions. Mark Hochstrasser, Yale University School of Medicine, and Cynthia Wolberger, Johns Hopkins University School of Medicine, are acknowledged for providing plasmids and yeast strains. Our work is generously supported by the Deutsche Forschungsgemeinschaft (projects HO 2541/4-1, SO 271/6-1 and SFB 740/TP B05) and by the Israel Science Foundation (grant 786/08).

References

Alfassy, O.S., Cohen, I., Reiss, Y., Tirosh, B., and Ravid, T. (2013). Placing a disrupted degradation motif at the C terminus of proteasome substrates attenuates degradation without impairing ubiquitylation. J Biol Chem *288*, 12645-12653.

Bagola, K., von Delbruck, M., Dittmar, G., Scheffner, M., Ziv, I., Glickman, M.H., Ciechanover, A., and Sommer, T. (2013). Ubiquitin binding by a CUE domain regulates ubiquitin chain formation by ERAD E3 ligases. Mol Cell *50*, 528-539.

Bays, N.W., Gardner, R.G., Seelig, L.P., Joazeiro, C.A., and Hampton, R.Y. (2001). Hrd1p/Der3p is a membrane-anchored ubiquitin ligase required for ER- associated degradation. Nat Cell Biol *3*, 24-29.

Bazirgan, O.A., and Hampton, R.Y. (2008). Cue1p is an activator of Ubc7p E2 activity in vitro and in vivo. J Biol Chem *283*, 12797-12810.

Berndsen, C.E., Wiener, R., Yu, I.W., Ringel, A.E., and Wolberger, C. (2013). A conserved asparagine has a structural role in ubiquitin-conjugating enzymes. Nat Chem Biol *9*, 154-156.

Berndsen, C.E., and Wolberger, C. (2011). A spectrophotometric assay for conjugation of ubiquitin and ubiquitin-like proteins. Anal Biochem *418*, 102-110.

Biederer, T., Volkwein, C., and Sommer, T. (1997). Role of Cue1p in ubiquitination and degradation at the ER surface. Science *278*, 1806-1809.

Boban, M., Ljungdahl, P.O., and Foisner, R. (2015). Atypical ubiquitylation in yeast targets lysine-less Asi2 for proteasomal degradation. J Biol Chem *290*, 2489-2495.

Brown, N.G., Watson, E.R., Weissmann, F., Jarvis, M.A., VanderLinden, R., Grace, C.R., Frye, J.J., Qiao, R., Dube, P., Petzold, G.*, et al.* (2014). Mechanism of polyubiquitination by human anaphase-promoting complex: RING repurposing for ubiquitin chain assembly. Mol Cell *56*, 246-260.

Burr, M.L., van den Boomen, D.J., Bye, H., Antrobus, R., Wiertz, E.J., and Lehner, P.J. (2013). MHC class I molecules are preferentially ubiquitinated on endoplasmic reticulum luminal residues during HRD1 ubiquitin E3 ligase-mediated dislocation. Proc Natl Acad Sci U S A *110*, 14290-14295.

Butt, T.R., Khan, M.I., Marsh, J., Ecker, D.J., and Crooke, S.T. (1988). Ubiquitin-metallothionein fusion protein expression in yeast. A genetic approach for analysis of ubiquitin functions. J Biol Chem *263*, 16364-16371.

Chen, P., Johnson, P., Sommer, T., Jentsch, S., and Hochstrasser, M. (1993). Multiple ubiquitin-conjugating enzymes participate in the in vivo degradation of the yeast MAT alpha 2 repressor. Cell *74*, 357-369.

Christensen, D.E., Brzovic, P.S., and Klevit, R.E. (2007). E2-BRCA1 RING interactions dictate synthesis of mono- or specific polyubiquitin chain linkages. Nat Struct Mol Biol *14*, 941-948.

Cohen, I., Wiener, R., Reiss, Y., and Ravid, T. (2015). Distinct activation of an E2 ubiquitin-conjugating enzyme by its cognate E3 ligases. Proc Natl Acad Sci U S A *112*, E625-632.

Cox, J., and Mann, M. (2008). MaxQuant enables high peptide identification rates, individualized p.p.b.-range mass accuracies and proteome-wide protein quantification. Nat Biotechnol *26*, 1367-1372.

David, Y., Ziv, T., Admon, A., and Navon, A. (2010). The E2 ubiquitin-conjugating enzymes direct polyubiquitination to preferred lysines. J Biol Chem *285*, 8595-8604.

Deng, M., and Hochstrasser, M. (2006). Spatially regulated ubiquitin ligation by an ER/nuclear membrane ligase. Nature *443*, 827-831.

Erijman, A., Shifman, J.M., and Peleg, Y. (2014). A single-tube assembly of DNA using the transfer-PCR (TPCR) platform. Methods Mol Biol *1116*, 89-101.

Finke, K., Plath, K., Panzner, S., Prehn, S., Rapoport, T.A., Hartmann, E., and Sommer, T. (1996). A second trimeric complex containing homologs of the Sec61p complex functions in protein transport across the ER membrane of S. cerevisiae. EMBO J *15*, 1482-1494.

Fletcher, A.J., Mallery, D.L., Watkinson, R.E., Dickson, C.F., and James, L.C. (2015). Sequential ubiquitination and deubiquitination enzymes synchronize the dual sensor and effector functions of TRIM21. Proc Natl Acad Sci U S A *112*, 10014-10019.

Furth, N., Gertman, O., Shiber, A., Alfassy, O.S., Cohen, I., Rosenberg, M.M., Doron, N.K., Friedler, A., and Ravid, T. (2011). Exposure of bipartite hydrophobic signal triggers nuclear quality control of Ndc10 at the endoplasmic reticulum/nuclear envelope. Molecular Biology of the Cell *22*, 4726-4739.

Gauss, R., Sommer, T., and Jarosch, E. (2006). The Hrd1p ligase complex forms a linchpin between ER-lumenal substrate selection and Cdc48p recruitment. EMBO J *25*, 1827-1835.

Habeck, G., Ebner, F.A., Shimada-Kreft, H., and Kreft, S.G. (2015). The yeast ERAD-C ubiquitin ligase Doa10 recognizes an intramembrane degron. J Cell Biol *209*, 261-273.

Haglund, K., Sigismund, S., Polo, S., Szymkiewicz, I., Di Fiore, P.P., and Dikic, I. (2003). Multiple monoubiquitination of RTKs is sufficient for their endocytosis and degradation. Nat Cell Biol *5*, 461-466.

Hershko, A., and Ciechanover, A. (1998). The ubiquitin system. Annu Rev Biochem *67*, 425-479.

Hirsch, C., Gauss, R., Horn, S.C., Neuber, O., and Sommer, T. (2009). The ubiquitylation machinery of the endoplasmic reticulum. Nature *458*, 453-460.

Hoege, C., Pfander, B., Moldovan, G.L., Pyrowolakis, G., and Jentsch, S. (2002). RAD6-dependent DNA repair is linked to modification of PCNA by ubiquitin and SUMO. Nature *419*, 135-141.

Ishikura, S., Weissman, A.M., and Bonifacino, J.S. (2010). Serine residues in the cytosolic tail of the T-cell antigen receptor alpha-chain mediate ubiquitination and

endoplasmic reticulum-associated degradation of the unassembled protein. J Biol Chem *285*, 23916-23924.

Johnson, E.S., Bartel, B., Seufert, W., and Varshavsky, A. (1992). Ubiquitin as a degradation signal. In EMBO J (PO Box 1, Eynsham, Oxford OX8 1JJ, United Kingdom, Irl Press Ltd), pp. 497-505.

Kim, H.T., Kim, K.P., Lledias, F., Kisselev, A.F., Scaglione, K.M., Skowyra, D., Gygi, S.P., and Goldberg, A.L. (2007). Certain pairs of ubiquitin-conjugating enzymes (E2s) and ubiquitin-protein ligases (E3s) synthesize nondegradable forked ubiquitin chains containing all possible isopeptide linkages. J Biol Chem *282*, 17375-17386.

Komander, D., and Rape, M. (2012). The ubiquitin code. Annu Rev Biochem *81*, 203-229.

Kostova, Z., Mariano, J., Scholz, S., Koenig, C., and Weissman, A.M. (2009). A Ubc7p-binding domain in Cue1p activates ER-associated protein degradation. J Cell Sci *122*, 1374-1381.

Lenk, U., Yu, H., Walter, J., Gelman, M.S., Hartmann, E., Kopito, R.R., and Sommer, T. (2002). A role for mammalian Ubc6 homologues in ER-associated protein degradation. J Cell Sci *115*, 3007-3014.

Lester, D., Farquharson, C., Russell, G., and Houston, B. (2000). Identification of a family of noncanonical ubiquitin-conjugating enzymes structurally related to yeast UBC6. Biochem Biophys Res Commun *269*, 474-480.

Lorick, K.L., Jensen, J.P., Fang, S., Ong, A.M., Hatakeyama, S., and Weissman, A.M. (1999). RING fingers mediate ubiquitin-conjugating enzyme (E2)-dependent ubiquitination. Proc Natl Acad Sci U S A *96*, 11364-11369.

Mattiroli, F., and Sixma, T.K. (2014). Lysine-targeting specificity in ubiquitin and ubiquitin-like modification pathways. Nat Struct Mol Biol *21*, 308-316.

McDowell, G.S., and Philpott, A. (2016). Chapter Two - New Insights Into the Role of Ubiquitylation of Proteins. In International Review of Cell and Molecular Biology, W.J. Kwang, ed. (Academic Press), pp. 35-88.

Metzger, M.B., Liang, Y.H., Das, R., Mariano, J., Li, S., Li, J., Kostova, Z., Byrd, R.A., Ji, X., and Weissman, A.M. (2013). A structurally unique E2-binding domain activates ubiquitination by the ERAD E2, Ubc7p, through multiple mechanisms. Mol Cell *50*, 516-527.

Metzger, M.B., Pruneda, J.N., Klevit, R.E., and Weissman, A.M. (2014). RING-type E3 ligases: Master manipulators of E2 ubiquitin-conjugating enzymes and ubiquitination. Biochim Biophys Acta. *1843*, 47-60.

Meusser, B., and Sommer, T. (2004). Vpu-mediated degradation of CD4 reconstituted in yeast reveals mechanistic differences to cellular ER-associated protein degradation. Mol Cell *14*, 247-258.

Mirzaei, H., Rogers, R.S., Grimes, B., Eng, J., Aderem, A., and Aebersold, R. (2010). Characterizing the connectivity of poly-ubiquitin chains by selected reaction monitoring mass spectrometry. Mol Biosyst *6*, 2004-2014.

Neuber, O., Jarosch, E., Volkwein, C., Walter, J., and Sommer, T. (2005). Ubx2 links the Cdc48 complex to ER-associated protein degradation. Nat Cell Biol *7*, 993-998.

Ramanathan, H.N., Zhang, G., and Ye, Y. (2013). Monoubiquitination of EEA1 regulates endosome fusion and trafficking. Cell Biosci *3*, 24.

Rappsilber, J., Mann, M., and Ishihama, Y. (2007). Protocol for micro-purification, enrichment, pre-fractionation and storage of peptides for proteomics using StageTips. Nat Protoc *2*, 1896-1906.

Ravid, T., and Hochstrasser, M. (2007). Autoregulation of an E2 enzyme by ubiquitin-chain assembly on its catalytic residue. Nat Cell Biol *9*, 422-427.

Ravid, T., and Hochstrasser, M. (2008). Diversity of degradation signals in the ubiquitin-proteasome system. Nat Rev Mol Cell Biol *9*, 679-689.

Rodrigo-Brenni, M.C., and Morgan, D.O. (2007). Sequential E2s drive polyubiquitin chain assembly on APC targets. Cell *130*, 127-139.

Shevchenko, A., Tomas, H., Havlis, J., Olsen, J.V., and Mann, M. (2006). In-gel digestion for mass spectrometric characterization of proteins and proteomes. Nat Protoc *1*, 2856-2860.

Shimizu, Y., Okuda-Shimizu, Y., and Hendershot, L.M. (2010). Ubiquitylation of an ERAD substrate occurs on multiple types of amino acids. Mol Cell *40*, 917-926.

Sommer, T., and Jentsch, S. (1993). A protein translocation defect linked to ubiquitin conjugation at the endoplasmic reticulum. Nature.

Swanson, R., Locher, M., and Hochstrasser, M. (2001). A conserved ubiquitin ligase of the nuclear envelope/endoplasmic reticulum that functions in both ER-associated and Matalpha2 repressor degradation. Genes Dev *15*, 2660-2674.

Walter, J., Urban, J., Volkwein, C., and Sommer, T. (2001). Sec61p-independent degradation of the tail-anchored ER membrane protein Ubc6p. Embo J *20*, 3124-3131.

Wang, X., Herr, R.A., Rabelink, M., Hoeben, R.C., Wiertz, E.J., and Hansen, T.H. (2009). Ube2j2 ubiquitinates hydroxylated amino acids on ER-associated degradation substrates. J Cell Biol *187*, 655-668.

Wu, K., Kovacev, J., and Pan, Z.Q. (2010). Priming and extending: a UbcH5/Cdc34 E2 handoff mechanism for polyubiquitination on a SCF substrate. Mol Cell *37*, 784-796.

Xu, P., Duong, D.M., Seyfried, N.T., Cheng, D., Xie, Y., Robert, J., Rush, J., Hochstrasser, M., Finley, D., and Peng, J. (2009). Quantitative proteomics reveals

the function of unconventional ubiquitin chains in proteasomal degradation. Cell *137*, 133-145.

Ye, Y., and Rape, M. (2009). Building ubiquitin chains: E2 enzymes at work. Nat Rev Mol Cell Biol *10*, 755-764.

Yu, H., and Kopito, R.R. (1999). The role of multiubiquitination in dislocation and degradation of the alpha subunit of the T cell antigen receptor. J Biol Chem *274*, 36852-36858.

Figure legends

Figure 1. Distinct activities of Ubc6 and Ubc7 in the ubiquitylation of Doa10 substrates. (A) Degradation of Vma12-*DegAB* was monitored in the given yeast strains by a cycloheximide decay assay and immunoblotting with anti-FLAG antibodies. An immunoblot using antibodies against Glucose-6-phosphate Dehydrogenase (G6PD) serves as loading control. wt – *wild type*. The topology of Vma12-*DegAB* is shown in a cartoon. C' refers to the carboxy-terminus of the protein. **(B-D)** Vma12-*DegAB* (B) or Vma12-*DegAB*$_{DD}$ (C and D) were isolated from lysates of the given yeast strains by FLAG affinity precipitation and analyzed by immunoblotting using anti-Ub and anti-FLAG antibodies. Where indicated the given Ub variants were overexpressed from plasmids. Arrowheads indicate the position of mono-ubiquitylated species. The numbers on the right refer to the migration of standard proteins of known molecular weight in kDa.

Figure 2. *In vitro* ubiquitylation by Ubc6 and Ubc7. **(A-C)** Immunoblot analysis of *in vitro* ubiquitylation time course experiments containing Doa10R and Ubc7/Cue1ΔTM (**A**), Doa10R and Ubc6ΔTM (**B**) or Doa10R, Ubc6ΔTM and Ubc7/Cue1ΔTM (**C**). Ub blots depict overall Ub levels, containing free unanchored Ub

chains as well as conjugates to Doa10R and Ubc6ΔTM. Cross-reacting signals of antibodies are indicated with asterisks. **(D)** *In vitro* ubiquitylation reactions of Doa10R, Ubc6ΔTM and Ubc7/Cue1ΔTM with different Ub variants (Ub, Ub_{R48}, Ub_{R63} and Ub_{R11}). A control (lane 1) was incubated with catalytically inactive Ubc6 ($Ubc6_{S87}$ΔTM). Samples were analyzed by SDS-PAGE and immunoblotting with the indicated antibodies. wt – *wild type*.

Figure 3. Mutations in Doa10R differently affect Ubc6 and Ubc7 activity. (**A**) Clustal Omega (Sievers et al., 2011) sequence alignment of the Doa10 RING domain with human and yeast APC11. Identical residues are highlighted in yellow. Residues mutated to alanine are marked with red dots. **(B-D)** *In vitro* ubiquitylation reactions containing Doa10R variants (wt Doa10R, $Doa10R_{A41}$, $Doa10R_{A43}$, $Doa10R_{A73}$) with Ubc7/Cue1ΔTM (B), Ubc6ΔTM (C) or both E2 enzymes (D). The stimulation of Ubc7 by Doa10R variants was determined by quantifying the formation of unanchored Ub chains and normalized to the activity of Ubc7 in absence of Doa10R (B, lower panel). Error bars represent standard deviation of three independent experiments. All Doa10R variants were analyzed by circular dichroism spectroscopy to ensure proper folding (**Figure S3**).

Figure 4. Ubc7 attaches K48-pUb directly to mono-Ub on Doa10R. **(A)** Doa10R was incubated with Ub_{R48} or Ub_{R63} in the presence of Ubc6ΔTM-His_6 or $Ubc6_{S87}$ΔTM-His_6 as indicated. The Ubc6 variants were removed by TALON® resin and Ub with Ubc7/Cue1ΔTM were added to the reaction. The samples were then analyzed by immunoblotting with the given antibodies. Unspecific signals due to cross-reacting antibodies are labeled with asterisks. Ub blots to determine Ubc7 activity are shown in **Figure S4A**. (**B**) Doa10R was incubated with Ubc6ΔTM in presence of Ub and a

mono-ubiquitylated form Doa10R-Ub was purified. Subsequently, Doa10R-Ub was supplied with Ub_{R48} and Ubc7/Cue1ΔTM or Ubc6ΔTM and the reaction products analyzed by immunoblotting with the given antibodies. Of note, purified Doa10R-Ub contained minor amounts of double mono-ubiquitylated Doa10R, unmodified Doa10R and inactivated Ubc6ΔTM. (**C**) Di-ubiquitylated forms of Doa10R (Doa10R-Ub_2) from (**B)** were isolated from SDS gels and the amount of lysine 48-linked Ub (UbK48) or total Ub in relation to standard peptides was determined by mass spectrometry. Lane numbering refers to the experiment in (B). Each probe was measured three times, with two transitions monitored for each peptide. The results were averaged and the standard deviation of mean is shown (see also **Figure S4B**). (**D,E**) Degradation of Ub_{V76}-$Ubc6_{S87}$ (Ub-$Ubc6_{S87}$) (**D**) or $Ub_{R48,V76}$-$Ubc6_{S87}$ (Ub_{R48}-$Ubc6_{S87}$) (**E**) was monitored by cycloheximide decay assays in the given yeast strains. Immunoblots with antibodies against glucose-6-phosphate dehydrogenase (G6PD) serve as loading controls. Quantification of immunoblot signals is shown in **Figures S4D and S4E**. The topology of un-cleavable Ub (Ub_{V76}) fused to $Ubc6_{S87}$ is shown in a cartoon. C' refers to the carboxy-terminus of the protein.

Figure 5. Ubc6 targets amino acids containing hydroxyl groups. **(A)** *In vitro* ubiquitylation of Ubc6 variants (wt Ubc6ΔTM, $Ubc6_{A196}$ΔTM) with fluorescently labeled ubiquitin. Where indicated, samples were treated with 100 mM NaOH to hydrolyze ester linkages (lane 4, 6, 8). Reactions lacking ATP serve as controls (lane 1, 2). Samples were analyzed by immunoblotting or fluorescence scanning (Ub-Alexa488). **(B)** Mass spectrometric analysis of the serine ubiquitylation site on Ubc6ΔTM after incubation with Ub, E1 and ATP. Ubc6-Ub was isolated from Coomassie-stained gels and processed as described in the Methods section. The b- and y-fragmentation pattern of the tryptic peptide, spanning residues 194 to 206,

shows the formation of an ester bond between the serine side chain and the C-terminus of ubiquitin. The ubiquitylated peptide was recorded at 949.99 m/z with a pep score of 254.72. Identified fragment ions are shown in the fragmentation legend. The modified serine 196 is included in both the b- and the y-series of fragment ions. **(C)** Schematic drawing of the chemical structure of the ubiquitin-ester bond to the serine side chain at position 196 of Ubc6. **(D)** Cell lysate was prepared from strains expressing either wt Ubc6 or $Ubc6_{A196}$ and incubated with 150 mM NaOH, where indicated. Samples were probed for Ubc6 to detect mono-ubiquitylated species.

Figure 6. Ubc6 conjugation sites are spatially flexible. **(A)** Sequence of Sbh2 showing the position of lysine residues and the transmembrane domain. Lysine residues that were mutated to arginine residues (Sbh2Δ4K) are marked with red dots. The topology of Sbh2 is presented in a cartoon. C' refers to the carboxy-terminus of the protein. **(B,C)** Quantification of cycloheximide decay assays to monitor the turnover of Sbh2 (B) and Sbh2Δ4K (C) in cells deleted for *SSH1* (*ssh1*Δ). The error bars represent standard deviation of 3 independent experiments. Representative immunoblots are shown in **Figure S7A**. **(D)** Degradation of FLAG-tagged Sbh2 or Sbh2Δ4K and their Ub fusions was monitored by cycloheximide decay assays in *ubc6Δ* yeast cells. Immunoblots with antibodies against G6PD serve as loading controls. Quantification of immunoblot signals is given in **Figure S7B**. The topology of un-cleavable Ub (Ub_{V76}) fused to Sbh2 is shown in a cartoon. C' refers to the carboxy-terminus of the protein. **(E)** Immunoprecipitation of FLAG-Sbh2 and FLAG-Sbh2Δ4K from lysates derived of Δ*ssh1 rpt4R* yeast cells harboring deletions of the indicated genes. In all cells Myc-Ub was overexpressed. Immunoblots showing the input material are given in **Figure S7C**. **(F)** Immunoprecipitation of FLAG-Sbh2 and FLAG-Sbh2Δ4K from *ssh1*Δ yeast cells overexpressing Myc-Ub. Samples were split

to two and, where indicated, NaOH was added to the sample buffer prior to loading on gels (lanes 4-6). Control precipitations from cell extracts that do not contain FLAG-tagged proteins are shown in lanes 1 and 4. Immunoblots showing the input material are given in **Figure S7D**.

Figure 7. A model for the tandem activity of Ubc6 and Ubc7 at the Doa10 ligase. **(A)** In the initial step, Ubc6 attaches short Ub conjugates to lysine residues (K) but also to other amino acids like serine (S) or threonine (T) of Doa10 substrates (Priming). **(B)** These primary Ub molecules label polypeptides for subsequent conjugation of K48-pUb chains by Ubc7 (Elongation). **(C)** In some cases, when lysine residues are presented in an appropriate context, Ubc7 can directly add Ub to client molecules, which partly supersedes Ubc6 activity.

Supplemental Figure legends

Figure S1 related to Figure 1: (A) Vma12-*DegAB* was expressed from plasmids in *rpt4R* cells that were, where indicated, deleted for *UBC7* or overexpressing Ub_{R48}. Vma12-*DegAB* was isolated by FLAG affinity precipitation from cells grown at permissive temperature and analyzed by immunoblotting using the given antibodies. Please note: Cells overexpressing Ub_{R48} still contain residual amounts of *wild type* Ub, which facilitates the formation of oligo-Ub on substrates. Vma12-*DegAB* migrates slightly different on individual SDS-gel systems. **(B)** Vma12-*DegAB* was immunoprecipitated from given yeast strains and Ub-Ub linkages on the substrate were analyzed by mass spectrometry as described in “Experimental procedures”. The relative abundance of peptides originating from K11-, K48-, or K63-linked Ub in relation to the amount of labeled standard peptides is shown in bar graphs. Each

sample was measured three times, with two transitions monitored for each peptide. Mean values with the standard deviation of mean are given. A yeast strain containing no FLAG-tagged substrate served as loading control (ctrl). The amount of precipitated Vma12-*DegAB* is shown in an anti-FLAG immunoblot.

Figure S2, related to Figure 2. (A) Representative gels showing the purified components for the *in vitro* ubiquitylation assay by Coomassie staining. Bands corresponding to E1 and UBE2J2ΔTM are marked with an arrow. **(B)** Immunoprecipitation of Doa10R from ubiquitylation reactions containing FLAG-Ub and indicated components at time points 0 and 20 min. A control (lane 5) was incubated without Doa10 antibody. Precipitates were analyzed by SDS-PAGE and immunoblotting with specific antibodies for Doa10 and FLAG. **(C)** *In vitro* ubiquitylation reaction of Doa10R and Ubc6ΔTM with different Ub variants (Ub, Ub_{R48}, Ub_{R63} and Ub_{R11}). A control (lane 1) was incubated with catalytically inactive Ubc6 ($Ubc6_{S87}$ΔTM). Samples were analyzed by SDS-PAGE and immunoblotting using appropriate antibodies. wt – *wild type*. (B and C) Unspecific signals due to cross-reacting antibodies are labeled with asterisks.

Figure S3, related to Figure 3. Circular dichroism spectrum of *wild type* (wt) Doa10R compared to spectra of the variants $Doa10R_{A41}$, $Doa10R_{A43}$ and $Doa10R_{A73}$. Wavelength scans were performed at 20 °C (Roehm and Berg, 1997).

Figure S4, related to Figure 4. (A) Immunoblots using anti Ub antibodies of the ubiquitylation reactions shown in **Figure 4A**. Left panel: reactions of the first incubation step and right panel: reactions of the second incubation step. Please note: Commercially available Ub_{R48} and Ub_{R63} already contained small amounts of di-Ub

(Bagola et al., 2013). Overall Ub conjugates catalyzed by Ubc7 are diminished when Doa10R was primed with Ub_{R48} in the first reaction due to incorporation of residual Ub_{R48} in poly-Ub chains. Additionally, Doa10R-Ub stimulates formation of unanchored Ub chains to higher extent as unmodified Doa10R, which matches previous observations (Buetow et al., 2015; Ranaweera and Yang, 2013). **(B)** Doa10R-Ub and Doa10R-Ub_2 from reactions described in **Figure 4B** were isolated from Silver-stained gels as indicated in the left panel. These samples were analyzed by mass spectrometry for peptides representing defined Ub-Ub linkage types. Relative abundance of the K11, K48 and K63 Ub-Ub specific peptides to isotopically labeled standards are presented. The overall amount of Ub in relation to a standard is also given. Bar graphs represent the average of three measurements, with two transitions monitored for each peptide and error bars depicting the standard deviation of mean. (**C**) Cycloheximide decay assay showing turnover of Ubc6 and $Ubc6_{S87}$. Immunoblots against G6PD serve as loading controls. **(D,E)** Quantification of cycloheximide decay assays presented in **Figures 4D and 4E**.

Figure S5. *In vitro* ubiquitylation experiment of UBE2J2ΔTM-HA_3 with Doa10R, Ubc7/Cue1ΔTM and fluorescently labeled Ub. Reactions were analyzed by SDS-PAGE, immunoblotting and fluorescence scanning.

Figure S6, related to Figure 5. (**A**) *In vitro* mono-ubiquitylation of Ubc6. E1, Ub and ATP were pre-incubated for 30 min and Ubc6 was then added to the reaction. At the given time points aliquots were removed, samples were split and either supplemented with water or with 100 mM NaOH to hydrolyze oxy-ester bonds. Analysis of the reaction was done by immunoblotting. The quantification represents the relative amount of Ubc6-Ub in relation to the overall intensity of the Ubc6 signal.

The amount of Ub on hydroxylated amino acids was calculated by subtracting the intensity of NaOH-resistant Ubc6-Ub signals from total Ubc6-Ub. Error bars represent standard deviation of mean from three independent experiments. (**B**) Cycloheximide decay experiment to monitor turnover of Ubc6 variants (wt Ubc6ΔTM, $Ubc6_{S87}$ΔTM, $Ubc6_{A196}$ΔTM). Experiments were performed in *ubc6*Δ strains, which were transformed with plasmids for the expression of the indicated Ubc6 variants. **(C)** Cycloheximide decay assay to monitor Sbh2 turnover in cells deleted for *UBC6* and expressing the given Ubc6 variants (wt, $Ubc6_{S87}$ΔTM, $Ubc6_{A196}$ΔTM). **(C,D)** Immunoblots against Sec61 serve as loading controls

Figure S7, related to Figure 6. (A) Representative immunoblots for cycloheximide decay assays to determine Sbh2 and Sbh2Δ4K degradation in *SSH1*-deleted cells. Quantification of several of such experiments is shown in **Figures 6B and 6C**. **(B)** Quantification of cycloheximide decay assays presented in **Figure 6D**. **(C)** Blots showing input material from FLAG-Sbh2 immunoprecipitation experiment in **Figure 6E**. **(D)** Input material of the FLAG-Sbh2 pull down experiment in **Figure 6F**. Lanes 1 and 4 show extracts derived from cells that do not contain FLAG-tagged proteins.

Table S1. Yeast strains used in this work

Table S2. Plasmids used in this work

Table S3. Sequence and Q1 and Q2 masses of peptides and the related isotopically labeled standards used to determine the relative amount of Ub-Ub linkage types by mass spectrometry.

Supplemental Tables

Table S1

Yeast strain	Relevant genotype	Reference
YTX949	*prc1-1*	(Bagola et al., 2013)
YTX996	Δ*ubc6::HIS3, prc1-1*	This study
YTX112	Δ*ssh1::HIS3*	This study
YTX113	Δ*ssh1::HIS3,* Δ*ubc7::LEU2*	This study
YTX131	Δ*ssh1::HIS3,* Δ*ubc6::LEU2*	This study
YAW032	Δ*ssh1::HIS3,* Δ*doa10::kanMX6*	This study
YTX127	Δ*ssh1::HIS3,* Δ*sbh2::TRP1*	This study
YTX126	Δ*ssh1::HIS3,* Δ*sbh2::TRP1,* Δ*ubc7::LEU2*	This study
YAW065	Δ*ssh1::HIS3,* Δ*sbh2::TRP1,* Δ*ubc6::HIS3*	This study
YAW067	Δ*ssh1::HIS3,* Δ*sbh2::TRP1,* Δ*doa10::kanMX6*	This study
YBM83	*rpt4R*	(Meusser et al., 2004)
YBM84	*rpt4R,* Δ*ubc7::LEU2*	(Meusser et al., 2004)
TRy171	Δ*doa10:HIS3*	(Swanson et al., 2001)
TRy1027	Δ*ubc6::HIS3*	This study
TRy1031	Δ*ubc6::HIS3* Δ*ubc7::LEU2*	This study
TRy1186	Δ*ubc7::LEU2*	This study
TRy1206	*his3-*Δ*200::pRS303::HIS*	This study
YAW072	Δ*ssh1::HIS3, rpt4R*	This study
YAW076	Δ*ssh1::HIS3,* Δ*ubc6::HIS3, rpt4R*	This study
YAW077	Δ*ssh1::HIS3,* Δ*ubc7::LEU2, rpt4R*	This study
YAW074	Δ*ssh1::HIS3,* Δ*doa10::kanMX6, rpt4R*	This study

Table S2

Plasmid	Plasmid backbone	Protein encoded by insert	Reference
Bacterial expression plasmids			
pTX249	pGEX-6p1	Ubc7 (2-165)	(Bagola et al., 2013)
pTX327	pGEX-6p1	Doa10R (2-125)	(Bagola et al., 2013)
pTX352	pQE60	Ubc6ΔTM-His_6 (1-230)	This study
pTX401	pQE60	$Ubc6_{S87}$ΔTM-His_6	This study
pTX410	pGEX-6p1	Cue1ΔTM-His_6 (24-203)	(Bagola et al., 2013)
pAW039	pGEX-6p1	Ubc6ΔTM (2-230)	This study
pAW128	pGEX-6p1	$Ubc6_{A196}$ΔTM	This study
pAW133	pGEX-6p1	UBE2J2ΔTM (1-235)	This study
pMD008	pGEX-6p1	Yeast Ub_{C20} S20C	(Bagola et al., 2013)
pTR1543	pET14	FLAG-Ub	(Cohen et al., 2015)
pAW101	pGEX-6p1	$Doa10R_{A41}$	This study
pAW102	pGEX-6p1	$Doa10R_{A43}$	This study
pAW103	pGEX-6p1	$Doa10R_{A73}$	This study
pTX481	pET21d	Uba1-His_6	(Berndsen and Wolberger, 2011)
Yeast expression plasmids			
pAW123	pRS416	Sbh2	This study
pAW125	pRS416	$Sbh2_{R15\ R23\ R25\ R28}$	This study
pTR1646	pRS414	FLAG-Sbh2	This study
pAW135	pRS414	FLAG-$Sbh2_{R15\ R23\ R25\ R28}$	This study
pAW027	pRS416	Ubc6	This study
pAW041	pRS416	$Ubc6_{S87}$	This study
pAW130	pRS416	$Ubc6_{A196}$	This study
pAW047	pRS424	Myc-Ub under CUP-Promoter	This study
pTR990	pRS317	Ub under CUP-Promoter	Mark Hochstrasser
pTR1173	Yep96	Ub_{R11} under CUP-Promoter	(Bagola et al., 2013)
pTR1171	Yep96	Ub_{R48} under CUP-Promoter	(Bagola et al., 2013)
pTR913	pRS414	Vma12-FLAG-*DegAB*	(Alfassy et al., 2013)
pTR1114	pRS414	Vma12-FLAG-$DegAB_{DD}$	(Alfassy et al., 2013)
pTR608	YCplac33	Ubc6	(Chen et al., 1993)
pTR1341	YCplac33	$Ubc6_{S87}$	This study
pTR1650	YCplac33	Ub_{V76}-$Ubc6_{S87}$	This study
pTR1681	YCplac33	$Ub_{R48,V76}$-$Ubc6_{S87}$	This study
pTR1688	pRS414	Ub_{V76}-FLAG-Sbh2	This study
pTR1694	pRS414	Ub_{V76}-FLAG-$Sbh2_{R15\ R23\ R25\ R28}$	This study

Table S3

Ub-Ub linkage	Sequence	Q1 mass	Q2 mass	Isotope
UbK11	TLTG[K-GG]TITLEVESSDTIDNVK	796.1 793.4 796.1 793.4	986.5 978.5 1115.5 1107.5	K8 K0 K8 K0
UbK48	LIFAG[K-GG]QLEDGR	490.9 487.6 490.9 487.6	622.8 617.8 357.2 347.2	R10 R0 R10 R0
UbK63	TLSDYNIQ[K-GG]ESTLHLVLR	752.1 748.7 752.1 748.7	1020.5 1015.5 1077.6 1067.6	R10 R0 R10 R0
Ub total	EGIPPDQQR	525.3 520.3 525.3 520.3	750.4 740.4 653.3 643.3	R10 R0 R10 R0

References for Supplemental Tables

Alfassy, O.S., Cohen, I., Reiss, Y., Tirosh, B., and Ravid, T. (2013). Placing a disrupted degradation motif at the C terminus of proteasome substrates attenuates degradation without impairing ubiquitylation. J Biol Chem *288*, 12645-12653.

Bagola, K., von Delbruck, M., Dittmar, G., Scheffner, M., Ziv, I., Glickman, M.H., Ciechanover, A., and Sommer, T. (2013). Ubiquitin binding by a CUE domain regulates ubiquitin chain formation by ERAD E3 ligases. Mol Cell *50*, 528-539.

Berndsen, C.E., and Wolberger, C. (2011). A spectrophotometric assay for conjugation of ubiquitin and ubiquitin-like proteins. Anal Biochem *418*, 102-110.

Chen, P., Johnson, P., Sommer, T., Jentsch, S., and Hochstrasser, M. (1993). Multiple ubiquitin-conjugating enzymes participate in the in vivo degradation of the yeast MAT alpha 2 repressor. Cell *74*, 357-369.

Cohen, I., Wiener, R., Reiss, Y., and Ravid, T. (2015). Distinct activation of an E2 ubiquitin-conjugating enzyme by its cognate E3 ligases. Proc Natl Acad Sci U S A *112*, E625-632.

Meusser, B., and Sommer, T. (2004). Vpu-mediated degradation of CD4 reconstituted in yeast reveals mechanistic differences to cellular ER-associated protein degradation. Mol Cell. *14*, 247-258.

Swanson, R., Locher, M., and Hochstrasser, M. (2001). A conserved ubiquitin ligase of the nuclear envelope/endoplasmic reticulum that functions in both ER-associated and Matalpha2 repressor degradation. Genes Dev *15*, 2660-2674.

Figure 1

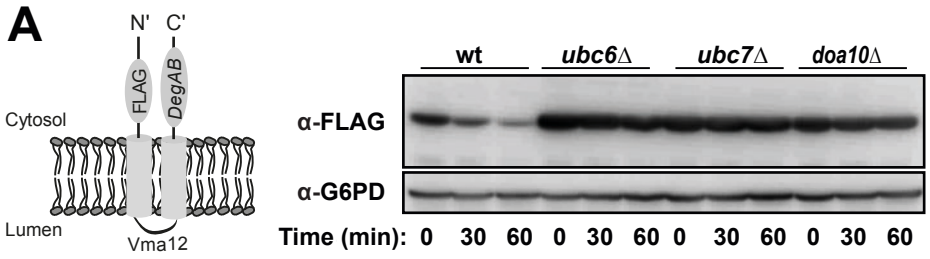
A
N'
C'
FLAG
DegAB
Cytosol
Lumen
Vma12
wt
ubc6Δ
ubc7Δ
doa10Δ
α-FLAG
α-G6PD
Time (min): 0 30 60 0 30 60 0 30 60 0 30 60

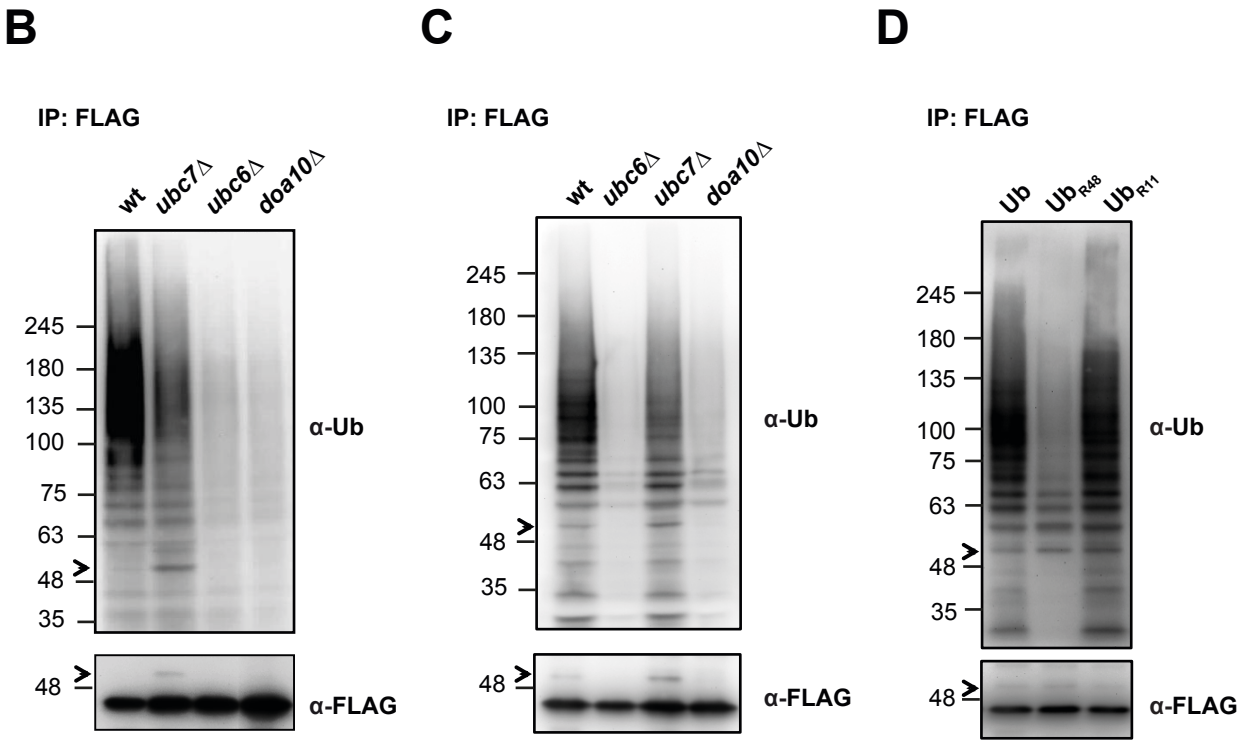
B
IP: FLAG
wt
ubc7Δ
ubc6Δ
doa10Δ
245
180
135
100
75
63
48
35
α-Ub
48
α-FLAG
C
IP: FLAG
wt
ubc6Δ
ubc7Δ
doa10Δ
245
180
135
100
75
63
48
35
α-Ub
48
α-FLAG
D
IP: FLAG
Ub
UbR48
UbR11
245
180
135
100
75
63
48
35
α-Ub
48
α-FLAG

Figure 2

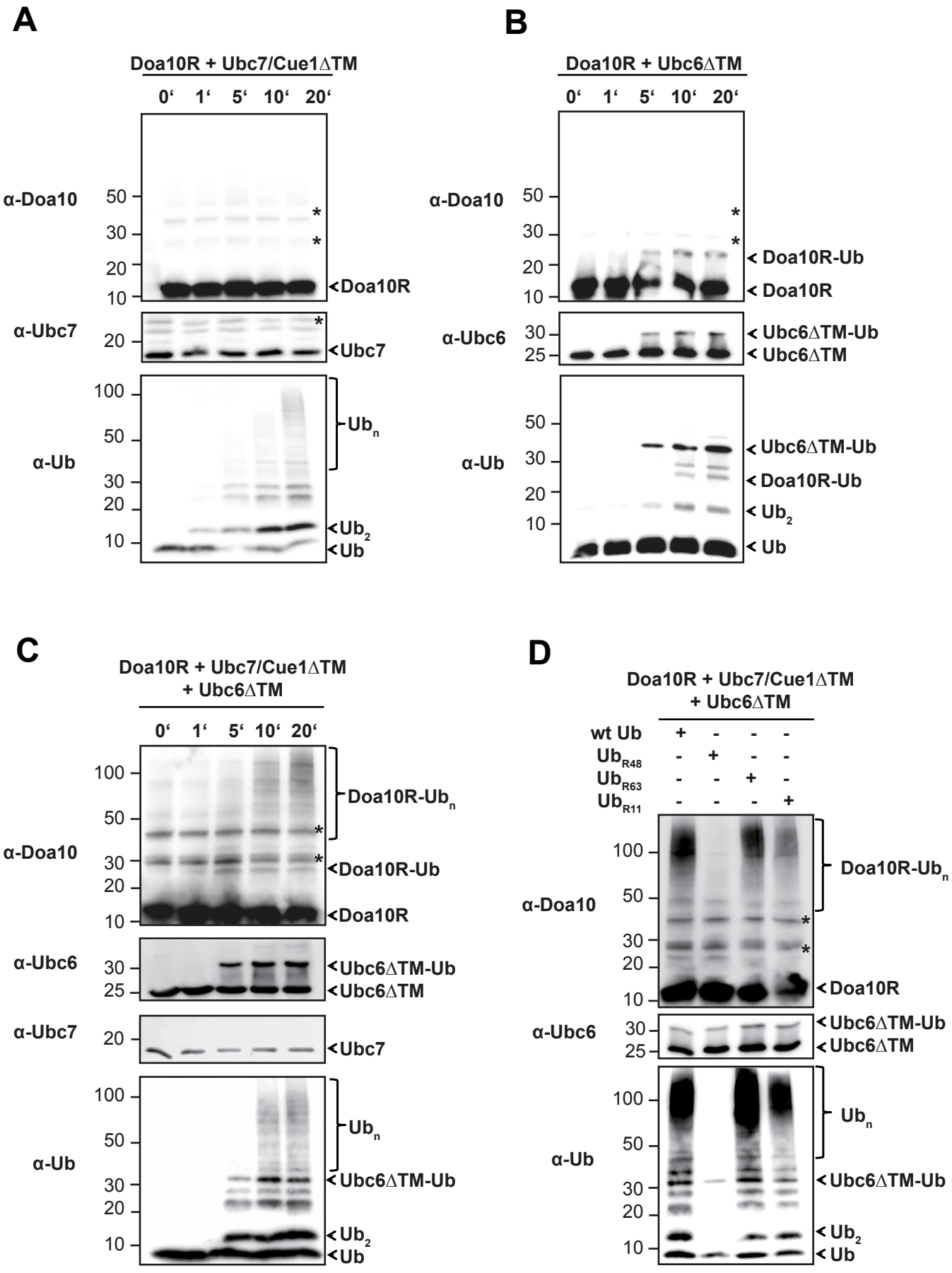
A
Doa10R + Ubc7/Cue1ΔTM
0‘ 1‘ 5‘ 10‘ 20‘
α-Doa10
50
30
20
10
*
*
Doa10R
α-Ubc7
20
*
Ubc7
100
50
30
20
10
α-Ub
Ub$_n$
Ub$_2$
Ub
B
Doa10R + Ubc6ΔTM
0‘ 1‘ 5‘ 10‘ 20‘
α-Doa10
50
30
20
10
*
*
Doa10R-Ub
Doa10R
α-Ubc6
30
25
Ubc6ΔTM-Ub
Ubc6ΔTM
50
30
20
10
α-Ub
Ubc6ΔTM-Ub
Doa10R-Ub
Ub$_2$
Ub
C
Doa10R + Ubc7/Cue1ΔTM
+ Ubc6ΔTM
0‘ 1‘ 5‘ 10‘ 20‘
100
50
30
20
10
α-Doa10
Doa10R-Ub$_n$
*
*
Doa10R-Ub
Doa10R
α-Ubc6
30
25
Ubc6ΔTM-Ub
Ubc6ΔTM
α-Ubc7
20
Ubc7
100
50
30
20
10
α-Ub
Ub$_n$
Ubc6ΔTM-Ub
Ub$_2$
Ub
D
Doa10R + Ubc7/Cue1ΔTM
+ Ubc6ΔTM
wt Ub + - - -
Ub$_{R48}$ - + - -
Ub$_{R63}$ - - + -
Ub$_{R11}$ - - - +
100
50
30
20
10
α-Doa10
Doa10R-Ub$_n$
*
*
Doa10R
α-Ubc6
30
25
Ubc6ΔTM-Ub
Ubc6ΔTM
100
50
30
20
10
α-Ub
Ub$_n$
Ubc6ΔTM-Ub
Ub$_2$
Ub

Figure 3

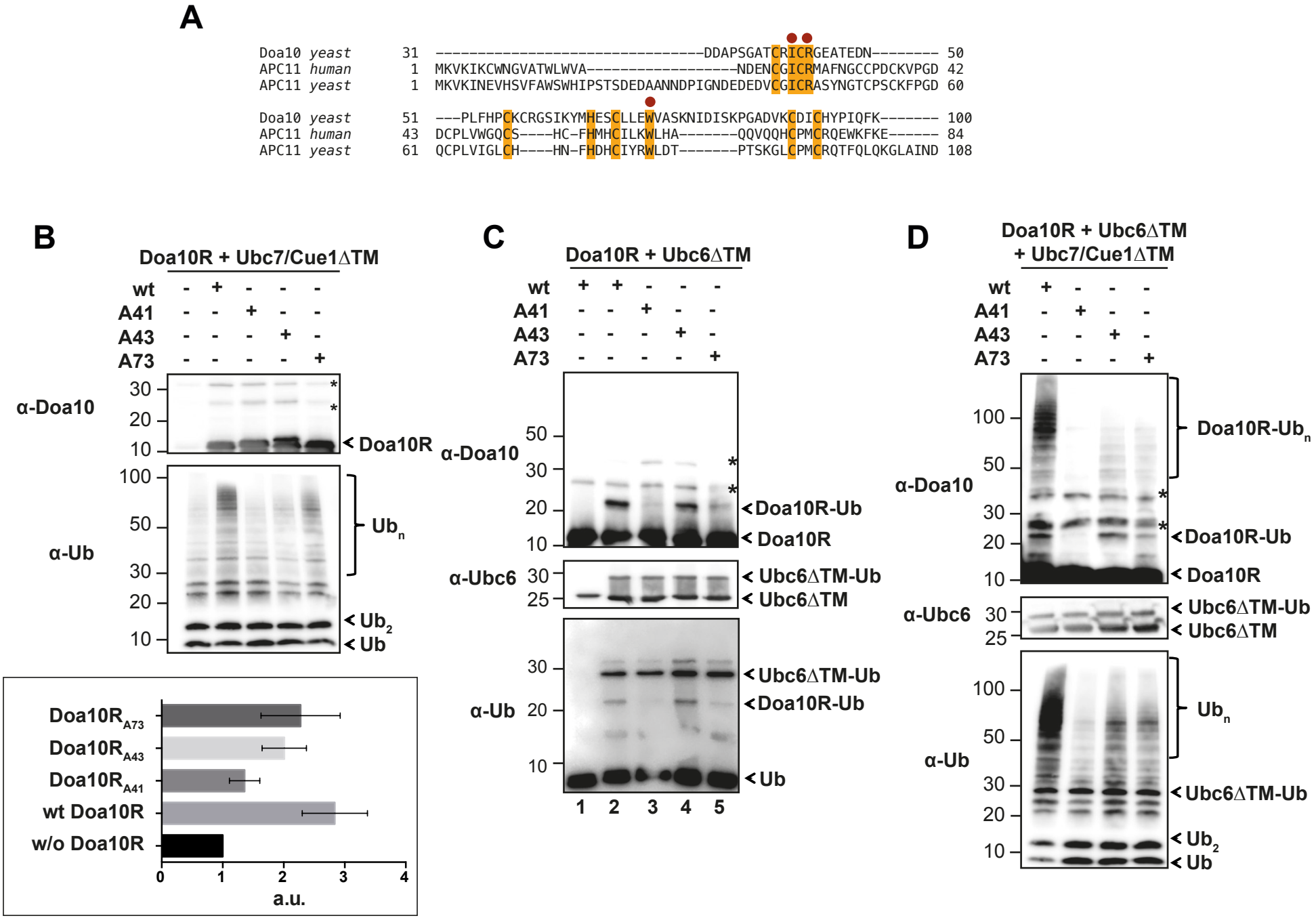
A
Doa10 yeast 31 ----------DDAPSGATCRICRGEATEDN-------- 50
APC11 human 1 MKVKIKCWNGVATWLWVA----------NDENCGICRMAFNGCCPDCKVPGD 42
APC11 yeast 1 MKVKINEVHSVFAWSWHIPSTSDEDAANNDPIGNDEDEDVCGICRASYNGTCPSCKFPGD 60
Doa10 yeast 51 ---PLFHPCKCRGSIKYMHESCLLEWVASKNIDISKPGADVKCDICHYPIQFK------- 100
APC11 human 43 DCPLVWGQCS----HC-FHMHCILKWLHA-------QQVQQHCPMCRQEWKFKE------ 84
APC11 yeast 61 QCPLVIGLCH----HN-FHDHCIYRWLDT-------PTSKGLCPMCRQTFQLQKGLAIND 108
B
Doa10R + Ubc7/Cue1ΔTM
wt
A41
A43
A73
α-Doa10
Doa10R
α-Ub
Ub_n
Ub_2
Ub
Doa10R_A73
Doa10R_A43
Doa10R_A41
wt Doa10R
w/o Doa10R
a.u.
C
Doa10R + Ubc6ΔTM
α-Doa10
Doa10R-Ub
Doa10R
α-Ubc6
Ubc6ΔTM-Ub
Ubc6ΔTM
α-Ub
Ub
D
Doa10R + Ubc6ΔTM
+ Ubc7/Cue1ΔTM

Figure 4

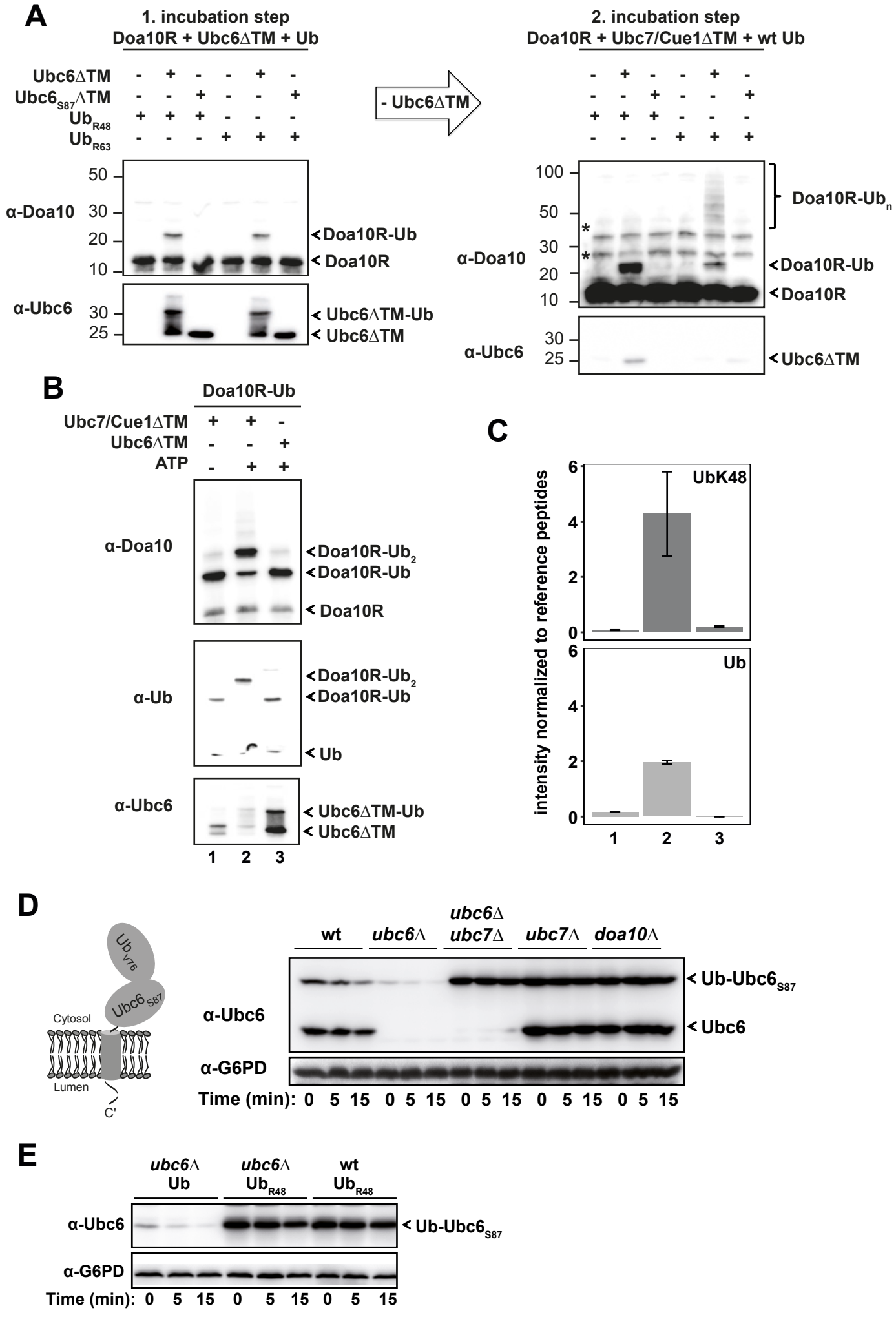
A
1. incubation step
Doa10R + Ubc6ΔTM + Ub
Ubc6ΔTM
Ubc6S87ΔTM
UbR48
UbR63
α-Doa10
Doa10R-Ub
Doa10R
α-Ubc6
Ubc6ΔTM-Ub
Ubc6ΔTM
- Ubc6ΔTM
2. incubation step
Doa10R + Ubc7/Cue1ΔTM + wt Ub
Doa10R-Ubn
B
Doa10R-Ub
Ubc7/Cue1ΔTM
Ubc6ΔTM
ATP
α-Doa10
Doa10R-Ub2
α-Ub
Ub
C
UbK48
Ub
intensity normalized to reference peptides
D
Ubv76
Ubc6S87
Cytosol
Lumen
C'
wt
ubc6Δ
ubc7Δ
doa10Δ
Ub-Ubc6S87
Ubc6
α-G6PD
Time (min): 0 5 15 0 5 15 0 5 15 0 5 15 0 5 15
E
ubc6Δ Ub
ubc6Δ UbR48
wt UbR48
Time (min): 0 5 15 0 5 15 0 5 15

Figure 5

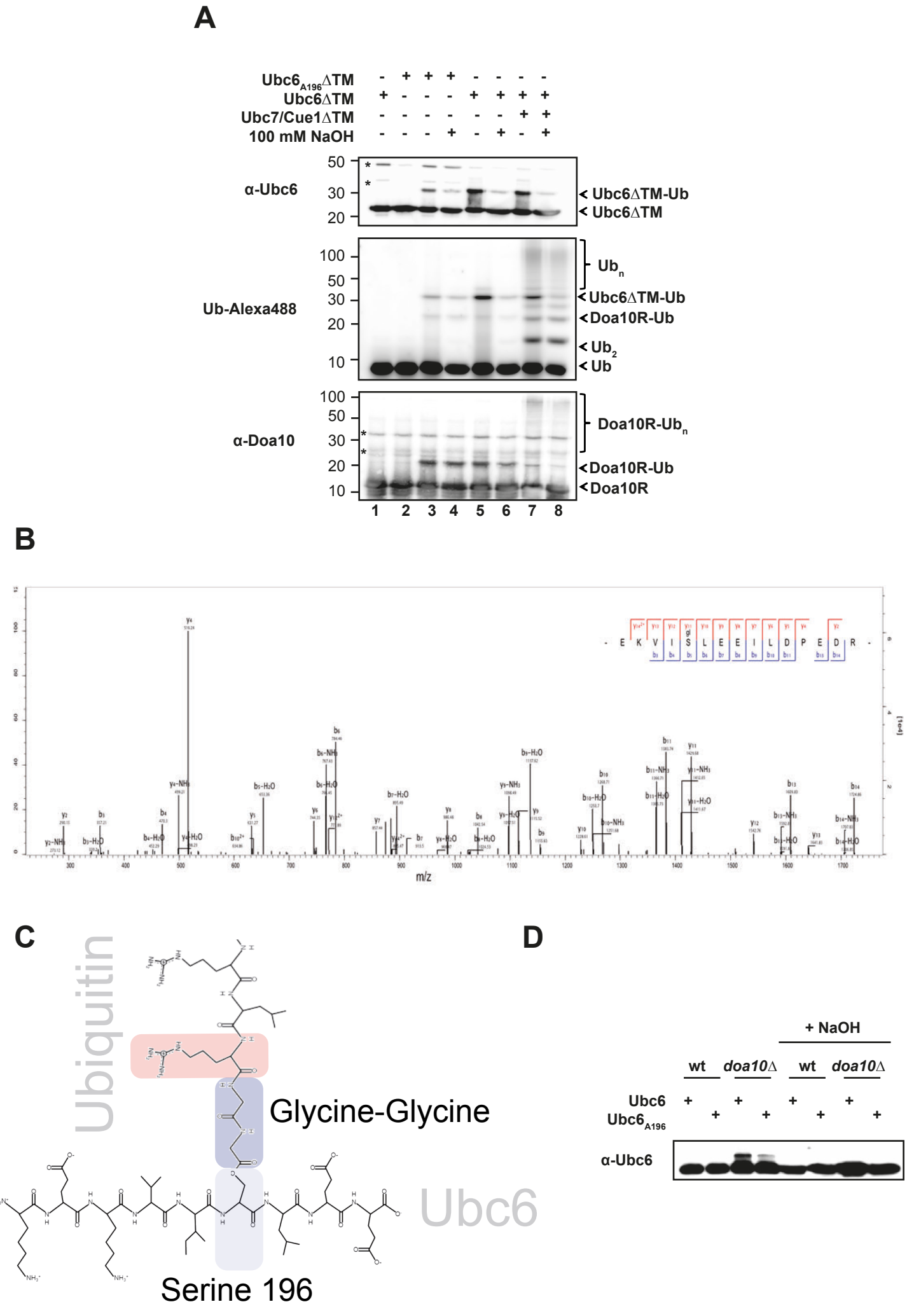
A
Ubc6A196ΔTM - + + + - - - -
Ubc6ΔTM + - - - + + + +
Ubc7/Cue1ΔTM - - - - - - + +
100 mM NaOH - - - + - + - +
α-Ubc6
50
30
20
Ubc6ΔTM-Ub
Ubc6ΔTM
Ub-Alexa488
100
50
30
20
10
Ubn
Ubc6ΔTM-Ub
Doa10R-Ub
Ub2
Ub
α-Doa10
100
50
30
20
10
Doa10R-Ubn
Doa10R-Ub
Doa10R
1 2 3 4 5 6 7 8
B
- E K V I S L E E I L D P E D R -
m/z
C
Ubiquitin
Glycine-Glycine
Ubc6
Serine 196
D
+ NaOH
wt
doa10Δ
wt
doa10Δ
Ubc6
Ubc6A196
α-Ubc6

Figure 6

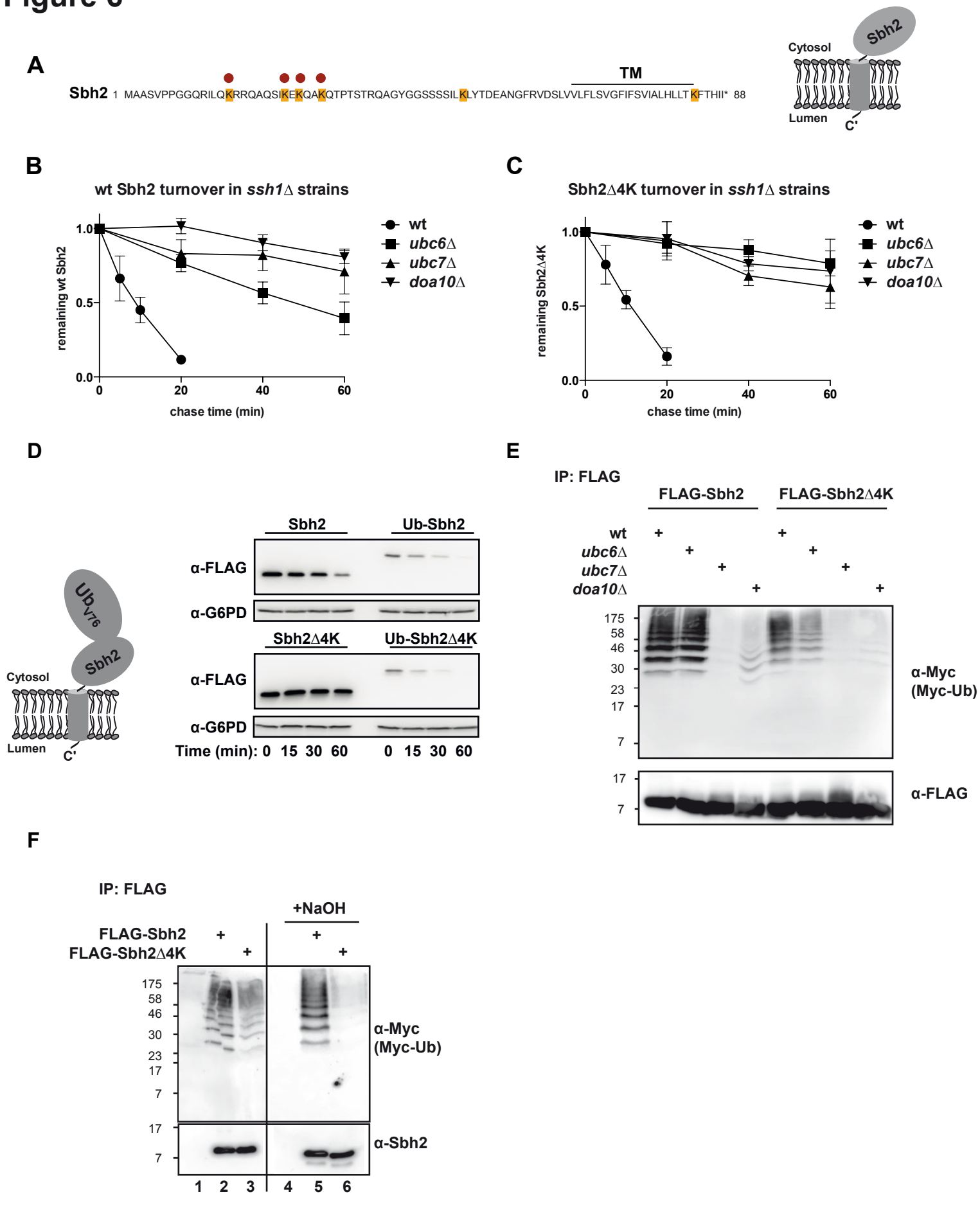
A
Sbh2 1 MAASVPPGGQRILQKRRQAQSIKEKQAKQTPTSTRQAGYGGSSSSILKLYTDEANGFRVDSLVVLFLSVGFIFSVIALHLLTKFTHII* 88
TM
Cytosol
Sbh2
Lumen
C'
B
wt Sbh2 turnover in ssh1Δ strains
remaining wt Sbh2
chase time (min)
wt
ubc6Δ
ubc7Δ
doa10Δ
C
Sbh2Δ4K turnover in ssh1Δ strains
remaining Sbh2Δ4K
chase time (min)
wt
ubc6Δ
ubc7Δ
doa10Δ
D
Ub
V76
Sbh2
Cytosol
Lumen
C'
Sbh2
Ub-Sbh2
α-FLAG
α-G6PD
Sbh2Δ4K
Ub-Sbh2Δ4K
α-FLAG
α-G6PD
Time (min): 0 15 30 60 0 15 30 60
E
IP: FLAG
FLAG-Sbh2
FLAG-Sbh2Δ4K
wt
ubc6Δ
ubc7Δ
doa10Δ
α-Myc
(Myc-Ub)
α-FLAG
F
IP: FLAG
+NaOH
FLAG-Sbh2
FLAG-Sbh2Δ4K
α-Myc
(Myc-Ub)
α-Sbh2
1 2 3 4 5 6

Figure 7

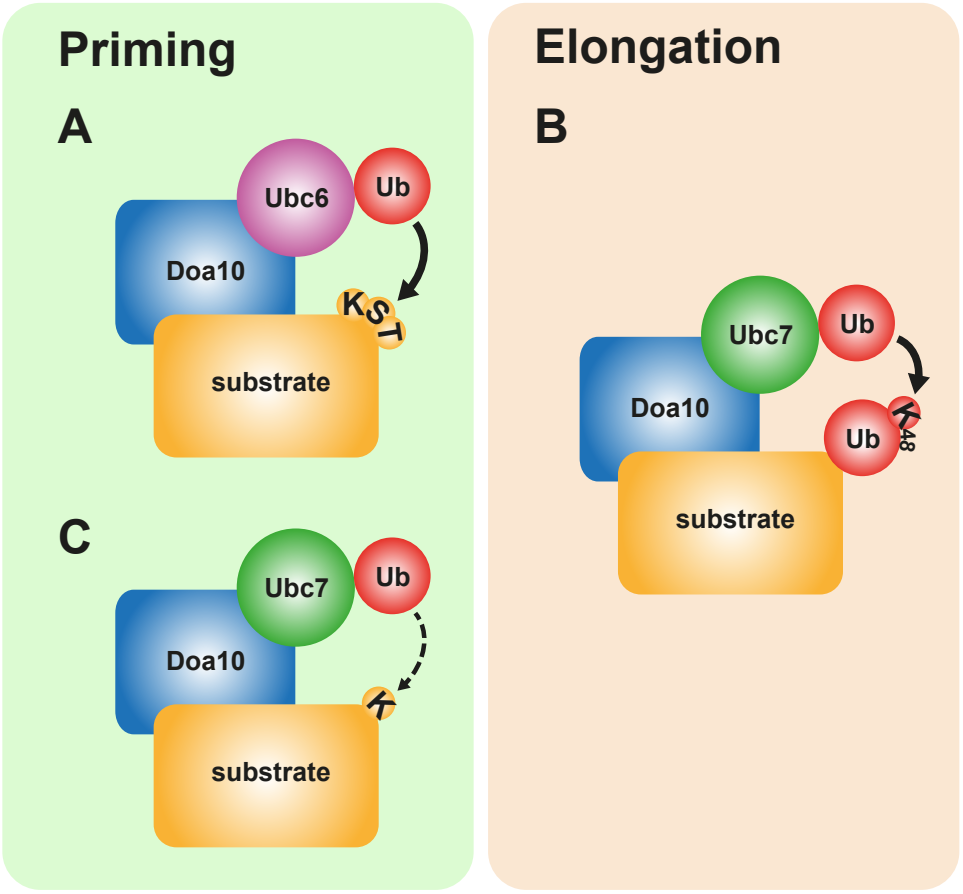
Priming
A
Ubc6
Ub
Doa10
K
S
T
substrate
C
Ubc7
Ub
Doa10
K
substrate
Elongation
B
Ubc7
Ub
Doa10
Ub
K48
substrate

Figure S1 (related to Figure 1)

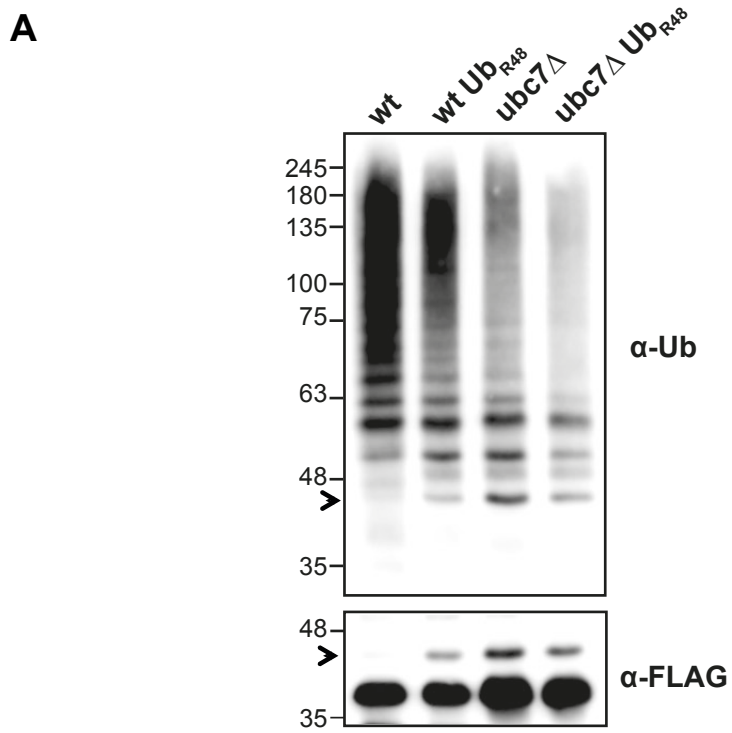

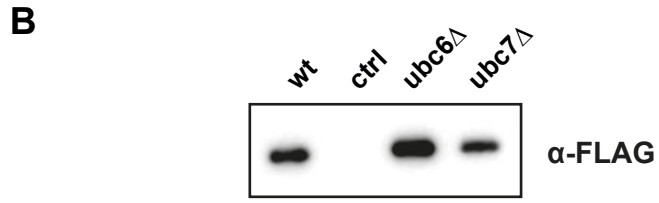

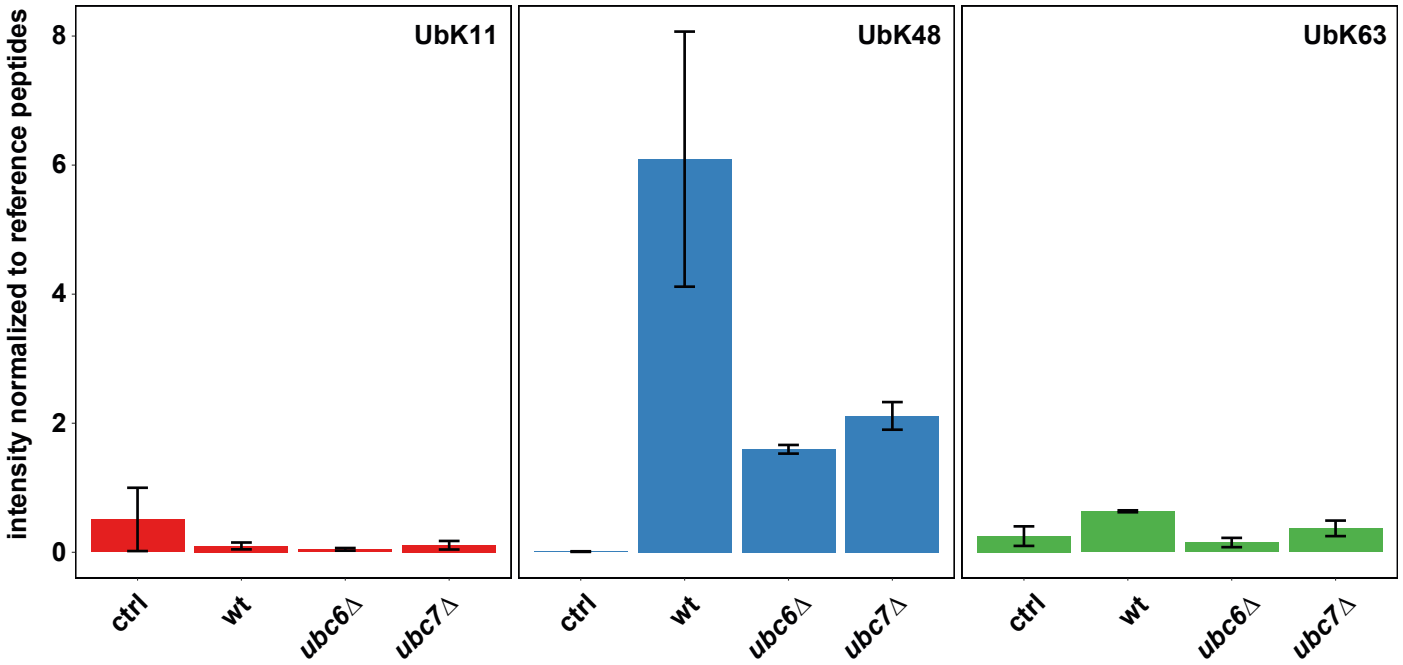

Figure S2 (related to Figure 2)

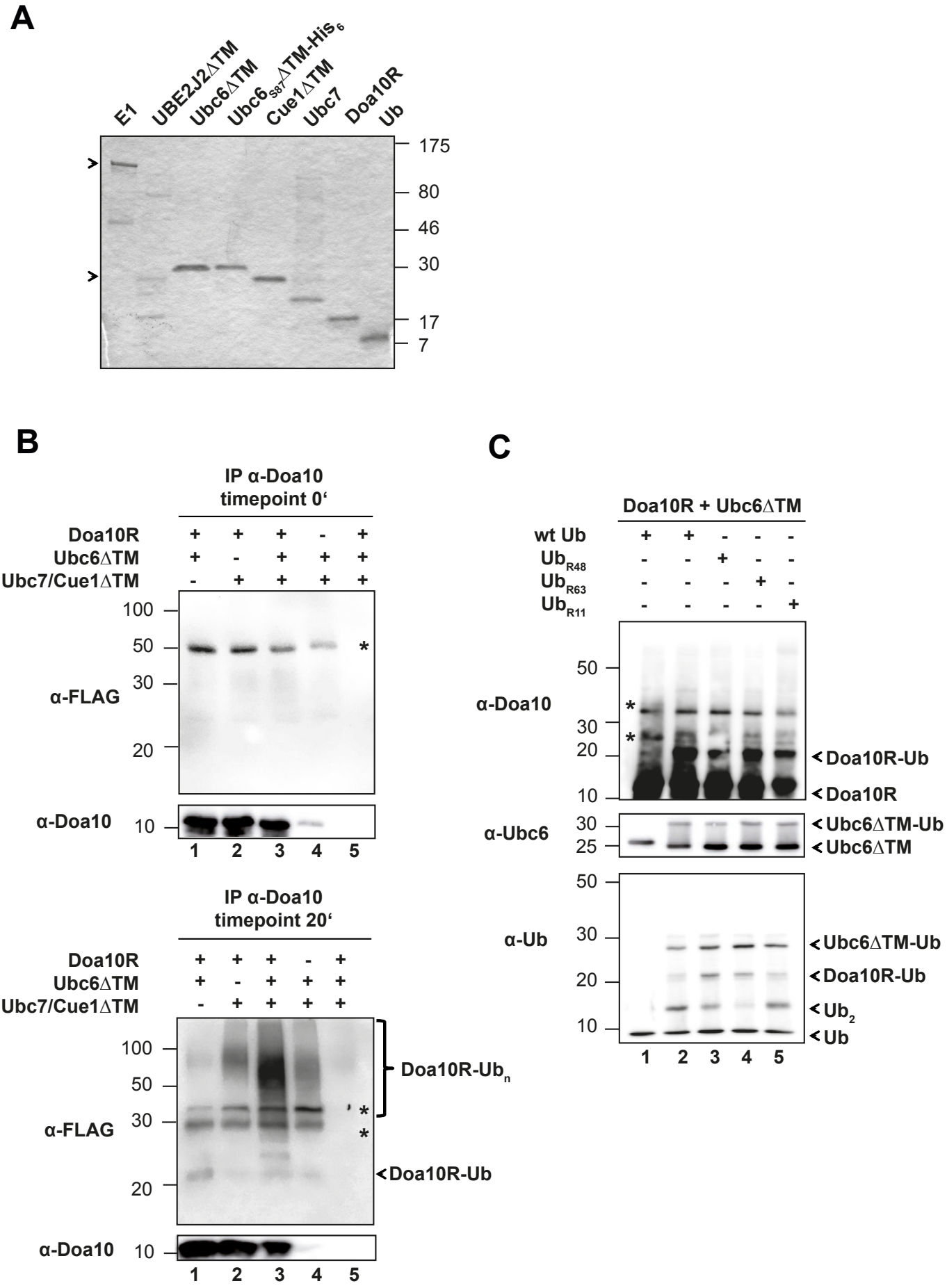

Figure S3 (related to Figure 3)

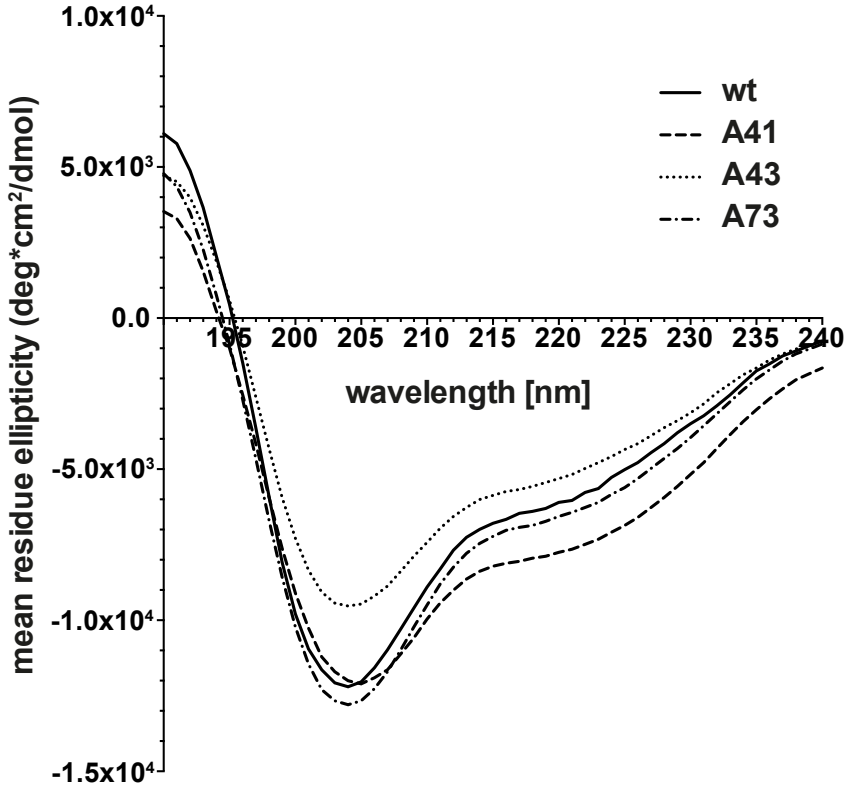

Figure S4 (related to Figure 4)

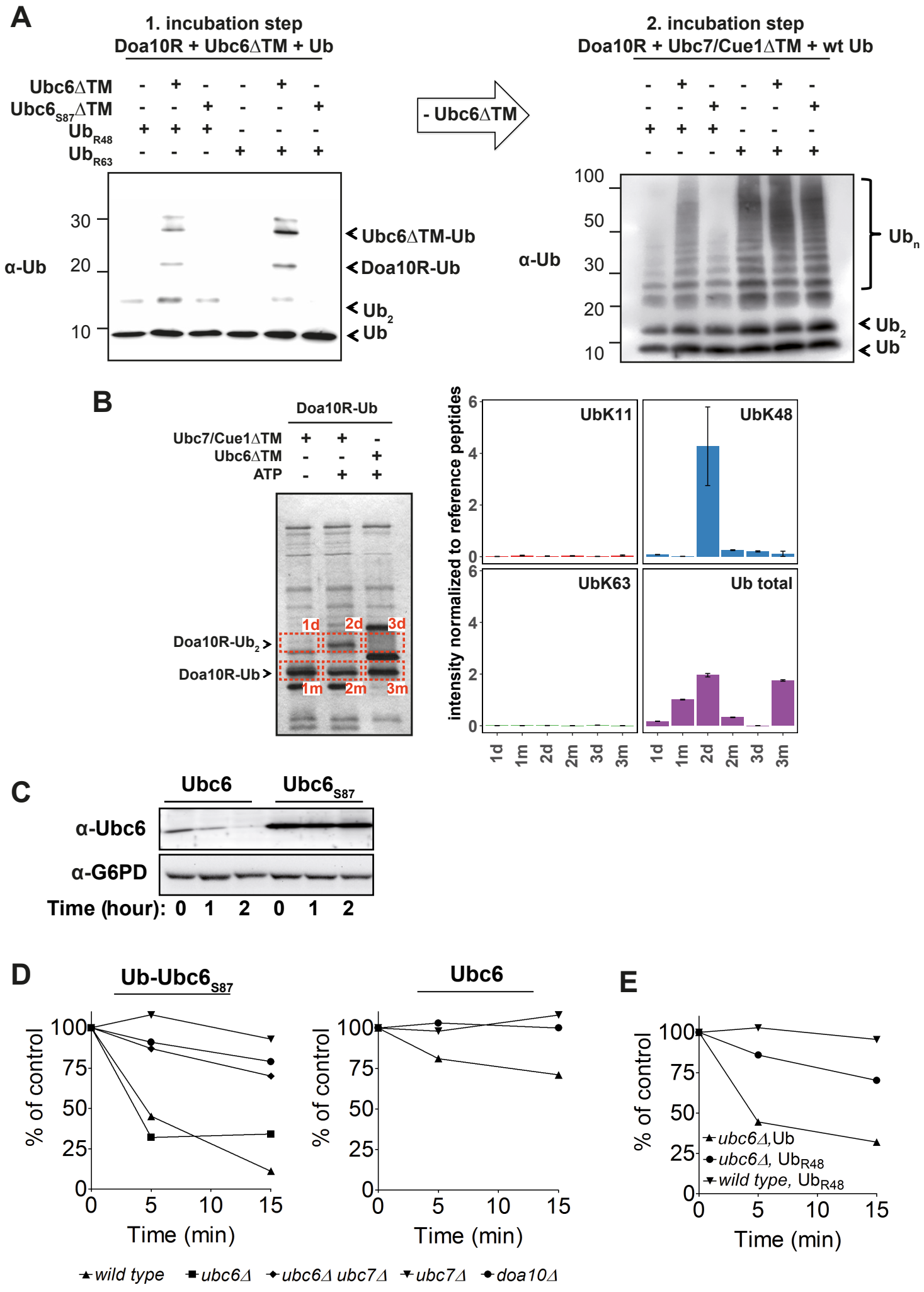

Figure S5

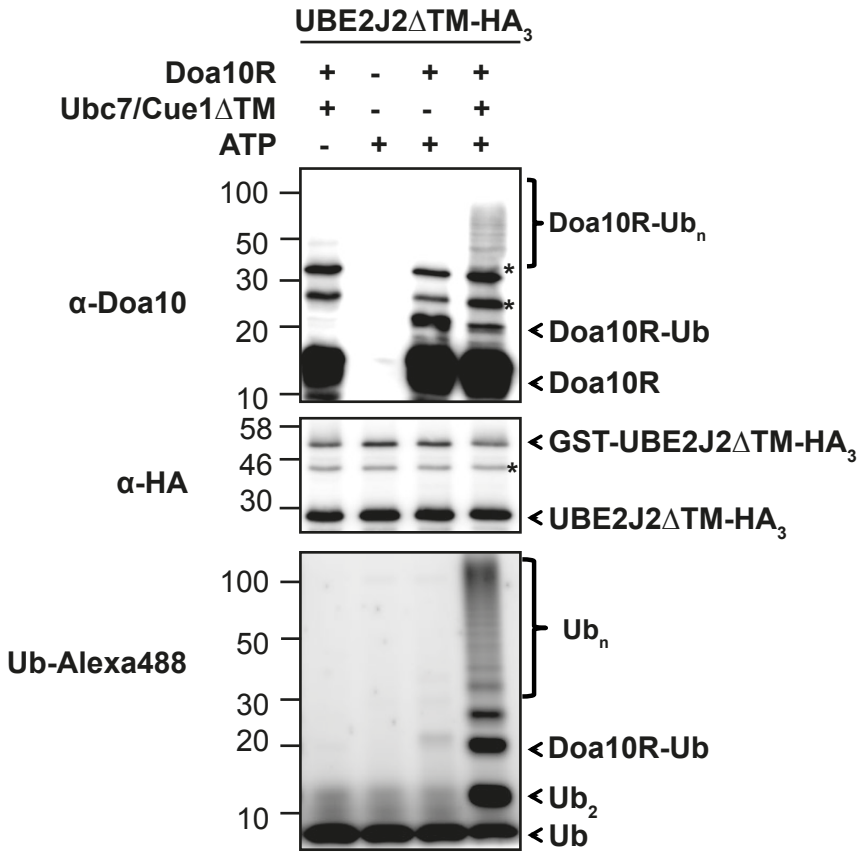
UBE2J2ΔTM-HA3
Doa10R + - + +
Ubc7/Cue1ΔTM + - - +
ATP - + + +
α-Doa10
100
50
30
20
10
Doa10R-Ubn
Doa10R-Ub
Doa10R
α-HA
58
46
30
GST-UBE2J2ΔTM-HA3
UBE2J2ΔTM-HA3
Ub-Alexa488
100
50
30
20
10
Ubn
Doa10R-Ub
Ub2
Ub

Figure S6 (related to Figure 5)

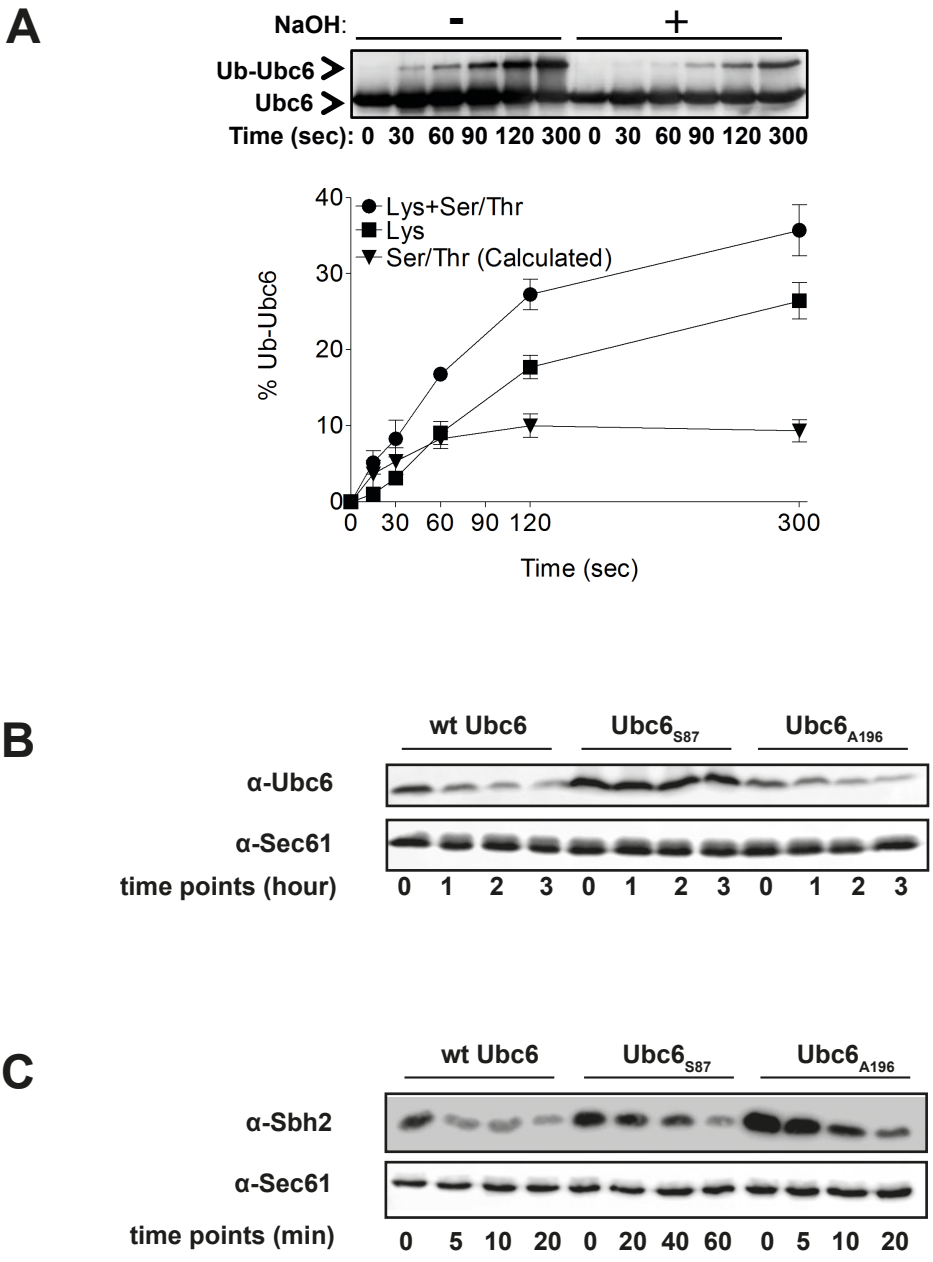

Figure S7 (related to Figure 6)